DYNAMIC RESPONSE OF PLATES TO BLAST LOAD

A Thesis Submitted
In Partial Fulfilment of the Requirements
for the Degree of
MASTER OF TECHNOLOGY

BY
A. RAJAMANI

to the

DEPARTMENT OF MECHANICAL ENGINEERING
INDIAN INSTITUTE OF TECHNOLOGY KANPUR
AUGUST 1972

TO MY PARENTS

CERTIFICATE

This is to certify that the thesis entitled "Dynamic Response of Plates to Blast Load" by A. Rajamani is a record of work carried out under my supervision and has not been submitted elsewhere for a degree.

V. SUNDARARAJAN
Associate Professor
Department of Mechanical Engineering
Indian Institute of Technology, Kanpur

August 11, 1972

ACKNOWLEDGEMENT

I am deeply indebted to Dr. V. Sundararajan for his guidance, encouragement and inspiration.

My thanks are also due to

Mr. K.S. Raghavan and Mr. B. Prasad for many interesting and fruitful discussions in the experiments.

Mr. M.M. Singh and Mr. Yadav for their continuous help in conducting the experiments.

Mr. J.D. Varma for his excellent typing.

Messors. D.K. Sarkar, T.M. Narasimhan, Nagaraj Murthy, R.K. Mallik, M.G. Subramaniam, T.K. Sadhukhan, Ajodhya Prasad and all others whose timely help made my task easier.

National Bureau of Standards (U.S. Department of Commerce) for supporting the work and financial assistance.

A. RAJAMANI

CONTENTS

LIST OF TABLES

LIST OF FIGURES

LIST OF PLATES

NOMENCLATURE

a	:	Plate length in x - direction
A_{mn}, A_m, A_n	:	Modal co-efficients
A_1	:	Area of the Plate without hole
A_2	:	Area of the hole in the plate
b	:	Plate length in y - direction
D	:	Flexural rigidity ($Eh^3/12\ (1-\nu^2)$)
e	:	Strain
$\bar{e}$	:	Strain in non-dimensionalised parameters
$f\ (P, t)$	:	Dynamic Pulse Load
$F.R$	:	Response Function
h	:	Plate Thickness
k_{ij}	:	Stiffness Co-efficients
L	:	Self adjacent differential operator
m	:	Mode number in n - direction
$M\ (P)$	:	Mass Distribution
M_{ij}	:	Mass Co-efficients
N_r	:	Generalised Force
n_r, q_r	:	Time Dependent Generalised Displacement co-ordinates.
n	:	Mode number in y - direction
P	:	Spatial Co-ordinates
R	:	a/b
s	:	Denotes Laplace Transform

t	:	The time variable
t_1, t_2, t_3	:	Pulse duration
T	:	Dimensionless time variable
w	:	Deflection of the Plate
W	:	Dimensionless deflection
W_{mm}	:	Natural frequency of the plate
$\bar{w}_{mm}$	:	Non - dimensionalised natural frequency
$W_{mm}(P)$	:	Admissible functions
$W(P)$	:	Absolute value of the functions
x, y	:	Position co-ordinates
X, Y	:	Dimensionless Position Co-ordinates
α	:	Frequency parameter
ψ	:	Resonance Frequency parameters
τ	:	Dummy Time variable
ν	:	Poisson's ratio
$\delta(P)$	:	Spatial dirac delta function
ρ	:	Density of the plate

SYNOPSIS

The response of plates with and without cut-outs to blast loading has been investigated experimentally in this work. In the theoretical analysis only plate without holes are considered.

Experiments have been conducted using shock tube as a loading medium. For plates without cut-outs dynamic strains are measured at the center and at the ends. Pressures are measured at different points to show the nature of the shock front. Similar measurements are made for plates with cut-outs and the dynamic strains for plates with and without cut-outs are compared at the ends. The variation of pressure distribution as a result of increase in the size of opening has been investigated. Results are given in terms of strains against area ratio and thickness to length of smaller edge ratio.

CHAPTER I

INTRODUCTION

1.1. General

The study of the effect of blast waves in the design of structures and equipments utilising plate components is becoming increasingly important for safer design. The buildings - industrial and domestic - should be able to withstand the pressure developed due to unexpected explosions (e.g. internal explosion due to cooking gas cylinder or air - blast from nuclear explosions[10] or conventional high explosives, such as TNT). The blast wave (a shock wave in air is referred to as a blast wave because it resembles and is accompanied by a very strong wind) may be strong enough to damage the walls, window panes etc. of the building. Sufficient experimental data are not available to estimate the load (and its nature) that is applied during an explosion or to predict the manner in which the structure responds.[17]

The study is receiving more attention with the introduction of supersonic air - crafts. When these crafts move at supersonic speed, a shock wave is generated and while reaching the ground, it interacts with the structures it encounters. The structure depending upon its relative orientation may be subjected to either a normal wave (when the normal of the wave front is in the direction of the displacement of the structural element) or a

travelling wave (when the normal of the wave front is parallel to the plane of the structural element). In actual practice, the nature of the shock wave is dependent upon a number of factors. In explosions, it depends on the presence of turbulence, the distance of the structural element from the place of explosion, the nature of explosion (nuclear, conventional explosion, gas explosion) The shock wave generarated from supersonic aircrafts depends on the atmospheric conditions, ground reflection etc. Therefore, it is extremely difficult to conduct experiments pertaining to actual conditions. Some experiments have been carried out to predict the nature of pressure distribution in shock wave in open air explosions.[10,11]

The idea of venting the walls - venting may be achieved by putting glass panels or weak windows which will be opened at an early stage so that other walls are not affected - has been thought[18] for explosion relief. But, to the best of the author's knowledge, no work has been done to predict the response of the structures and variation of pressure distribution with the openings present.

1.2. Previous Work

Most of the theoretical and experimental work in the literature have dealt with the response of beams and plates to blast loading.

The effect of shock wave on structures has been studied as a vibration problem subjected to a transient load. Frankland[1] solved this problem for rectangular and sine pulse for single degree of freedom systems and in the latter part of his paper he has given the outline to similar problems for continuous bodies.

Considerable amount of theoretical and experimental work has been done by Cheng[2], Baker[3], Banerjee[4], Symonds[5], Ting[6], Lee and Martin[7] on the dynamic response of elastic and plastic beams.

Dynamic response of circular plates to pulse loads has been dealt by George P.J.[8]. Wang[9] discussed the permanent deflection of a plastic plate under blast loading[9]. Florence[12] conducted experiments on simply supported circular plates subjected to uniformly distributed impulse and compared the permanent deformation with those predicted by bending theory of rigid plastic plates.

Jones[13] recently conducted experiments to study the behaviour of fully clamped plates subjected to uniformly distributed impulsive velocities. He developed

an approximate theoretical procedure to estimate the permanent transverse deflection of beams and plates when subjected to large dynamic loads.[14]

Influence of pulse shape on the final plastic deformation has been discussed by Youngdahl[15]. According to him, the amount of plastic deformation is dependent on the pulse shape for pulses which have the same impulse and maximum pressure. Allgood[16] considers loads of two types - short duration and long duration. He distinguishes long duration loads from short duration loads as being those with a duration t', greater than six times the natural period of the system under consideration. He concludes that peak loads with magnitudes of several times the yield load can be sustained if the load is of short duration. Moreover, he comments that if the ratio of the rise time to the natural period is less than one fifth, the load can be assumed to have an instantaneous rise and if the ratio is greater than 6, the load can be considered as static.

Cheng and Benveniste[19] solved the problem of dynamic response of structural elements exposed to shock waves. Both normal and travelling shock waves have been considered in their analysis.

Crocker[20] gave the theoretical results for the effect of travelling shock wave on a plate. The nature of shock wave was N. shaped in his problem. He gave the experimental verification for the above problem.

Damage due to sonic booms have been studied by Clark, Berr and Nexsen[23]. In their experiments they found out that the overpressures were not of sufficient magnitude to cause any structural damage to buildings that were properly constructed and well maintained. However, they found out that in some instances the structures investigated had an inner window cracked where as the storm window was not damaged.

Savin[21] has solved the problem of stress concentration around holes in infinite plates subjected to bending. Paramsivam[22] has used finite difference method to find out the static deflection and natural frequency of plates with rectangular holes. But he has given the results only for square plates with square and circular holes.

1.3. Present Work

From the literature survey, it seems that very few experimental results have been reported on the dynamic response of structural elements other than beams due to blast loading. Also the response of structures with

vents and subjected to shock loading has not been studied. The change in the pressure distribution as a result of the different shapes and sizes of vents has also not been considered. An attempt has been made to fill the above two gaps.

The existing shock tube was used for the present experimental study. The shock wave impinging on the plate was plane in all cases. The clamped plates with and without holes were exposed to normal shock wave. The dynamic strains at the center (for plate without holes), near the holes and at the ends were measured.

The experimental values for clamped plates without holes are checked with theoretical results. The analysis has been done within elastic limit and small deflection theory has been assumed. For simplicity, the damping has not been considered.

The analysis of rectangular plates with holes has not been considered because of the following reasons:

1. It is very difficult to know the exact functions which satisfy the boundary conditions near the hole and at the ends where the plates are either simply supported or clamped.

2. The computations involved even in case of static response or free vibrations of plates are enormous.[21,24]

The results for the variations in pressure distribution due to different vent size and shapes has been given. The response has been given in terms of dynamic strains.

Chapter II and III discuss experimental arrangements and analytical formulation respectively. Chapter IV and V discusses the results and scope for further work respectively.

In Appendices the response functions and static response have been given.

CHAPTER II

EXPERIMENTAL SET - UP

The experimental work has been carried out to find out the effect of shock loading on plates with and without holes and also to study the variation in the pressure distribution with the sizes of cut - outs. Experimental set up and procedure has been described in this chapter.

2.1 Shock - Tube and Production of Shock Wave

A shock - tube is a long chamber of constant cross - section which has two chambers - the high pressure and the low pressure separated by a diaphragm. The diaphragm can be ruptured to produce a shock wave which passes down the tube.

The shock tube used is of rectangular cross - section. The high pressure chamber is 6" x 4" in cross-section and 36" long. The low pressure side has five sections each 28" long and 6" x 4" cross - sections. The rectangular section is made of four different aluminium plates.

The different sections (on low pressure side) are joined by means of flanges and made air-tight with rubber gasket provided in between them. The high pressure

and low pressure sides are joined by a circular flange with provision for two O - rings. On the high pressure side, an inlet valve for filling it with compressed air and a Bourdon's pressure gage to read the pressure are provided.

To start the experiment, first the alignment of the shock tube is checked. To produce a shock - wave, the diaphragm (Cellophane paper has been used as diaphragm) is kept between the two chambers and then both sides are joined. Then the high pressure chamber is pressurised by means of compressed air to the desired pressure. The diaphragm is punctured at the center by means of a high resistance wire carrying high current. This causes the sudden rapture of the diaphragm.

The pressure - time record of the shock wave was found with the help of pressure transducers (Kistler type 623 B/ 601 A).

2.2 Measurement of Pressure

In order to know the exact pressure distribution on the plate, a stiff plate, considerably stiffer than the test plate, was used. It was mounted in the same position as the test plate. The pressure - transducer was mounted on this stiff plate. This is done for two reasons:

1. The vibration of the plate should not affect the signal of the transducer.

2. The pressure inside the shock - tube may be different than at the end where the plate is mounted. The pressure transducer gives pressure which acts on the plate.

The transducers used were of piezo - electrical crystal type which give a charge output proportional to pressure. The charge output is converted to voltage and amplified by means of a charge amplifier (Kistler - type 566 M3). The pressure signal from the charge amplifier is fed into a storage oscilloscope (Tektronix - type 564). The pressure measuring device has a rise - time of few micro seconds and a band width of several mega cycles. Since the rise time and duration of the pulse are of the order of milli seconds, the transducers were sufficient for the purpose used.

2.3 Measurement of Strain

The strain signals are found by means of strain rosettes. However for plates with holes (for ratio of plate size to hole - size 4) rosettes could not be used, due to the large size of rosettes. For such plate, single element gauges were used. As the duration of the

shock load is of the order of milli seconds, the strain rosettes and gauges are quite suitable for the measurement of dynamic strain.

In the case of plates, without holes, the rosettes were mounted at the ends and at the center. For plates with cut - outs of different sizes, rosettes were mounted near the holes and at the ends.

Temperature compensation was done by using dummy gauges mounted on a plate of same material.

The leads from the strain - gauges were connected to the Budd - Indicator. Full - bridge circuit was used for rosettes and half - bridge circuit for single element gauges. The output from the Budd Indicator was fed to the storage - oscilloscope. In this case oscilloscope was triggered by the signal from the pressure - transducer mounted on the wall of the shock - tube (fixed in adaptors which were cushioned in a packing material). A signal starting from zero can be stored on the storage oscilloscope due to this triggering arrangement.

2.4 Strain - Gauge Calibration

The calibration method consisted of determining the system's response to the introduction of a known small resistance change at the gauge and of calculating an equivalent strain there from. This change

in resistance was produced by means of a parallel resistor.

Let R_g = gauge resistance

R_c = calibration resistance

F = gauge factor

e = equivalent strain

The change in resistance is

$$\Delta R = \frac{R_g^2}{(R_g + R_s)}$$

$$e = \frac{\Delta R}{F\,(R_g)}$$

$$e = \frac{R_g}{F\,(R_g + R_s)} \qquad (2.4.1)$$

If there are N active gauges, then

$$e = \frac{1}{F}\,\frac{R_g}{N\,(R_g + R_s)} \qquad (2.4.2)$$

2.5 Clamping Arrangement

The plates were clamped at the end of the shock tube by means of two supporting frames. One supporting frame was rigidly fixed to the shock tube. The test plate was rigidly clamped to this supporting frame with the help of another frame and bolts. b/a is kept constant.

Equal tightning of the bolts was achieved by means of a torque wrench. The clamping arrangement is shown in Figure 6.

2.6 Specifications of the Instruments Used :

1. Strain Gauges

(a) CT - 3

Nominal gauge length	- 3.0 m.m.
Nominal width	- 2.0 m.m.
Base length	- 10.0 m.m.
Base width	- 5.0 m.m.
Resistance	- 120 ± 0.4 ohms.
Type	- Helical Grid
Gauge Factor	- 1.98 ± 0.2%

Rohits and Company (India)

(b) KWR - 5 R

Nominal gauge length	- 5.0 m.m.
Nominal width	- 4.0 m.m.
Base length	-22.0 m.m.
Base width	-22.0 m.m.
Resistance	- 110 ± 0.4 ohms
Type	- Helical rosette 45°
Gauge Factor	- 2.72 ± 0.2%

Rohits and Company (India)

2. Digital Strain Indicator (Portable, P - 350)

1.	Range	- ± 50,000 microstrain
2.	Accuracy	- ± 0.1 percent of reading or 5 microstrain for R = 120 ohms and G.F. = 2.00. For 50 to 2000 - ohm bridges, G.F. from 1.5 to 4.5, accuracy shall be 0.5 percent of reading or 5 microstrain.
3.	Readability	- 1 microstrain
4.	Balance	- 10 turn lock knob provides approximately ± 2000 microstrain (G.F. 2.00) for zeroing the digital readout prior to load application.
5.	Gage Factor	- From 0.10 to 10.00 (Calibrated between 1.50 and 4.50 only)
6.	External Circuits	- Full, Half, or Quarter Bridge; Internal dummy gauge for 120 and 350 ohm.
7.	Lead Wire Capicitance effect.	- Typically less than .05%. Negligible effect with 500 ft of lead wire.

8. Oscilloscope Jack - Full Scale ± 200 mv D.C. Sensitivity variable from approximately 0.4 to 20 μc/mv.

9. Battery - 9 volts

The Budd Company, Instruments Division (U.S.A)

3. Pressure - Transducer

Model - 601 A/623 B

Pressure Range	-	Full vaccum to 3000 psi
Resolution	-	0.1 psi
Maximum Pressure	-	5000 psi
Sensitivity (nominal)	-	1 picocoulomb/psi
Resonant frequency	-	130,000 cps
Rise time	-	3 micro-seconds
Linearity	-	1 percent
Acceleration sensitivity	-	0.01 psi/g
Temperature range	-	-450 to + 500 °F
Shock and Vibration	-	15,000 g's
Sensing element	-	Crystalline quartz

KISTLER INSTRUMENT CORPORATION (U.S.A.)

4. Charge - Amplifier

Model - 566

Ranges (for + 10 volts or ± 5 volts output)	-	0.05, 0.1, 0.2, 0.5, 1.0, 2.0, 5.0, 10.0, 20.0, 50.0, and 100 mv/pcb.
Output voltage (to high impedance load)	-	+ 10 volts, - 5 volts
Output current (to low impedance load)	-	± 10 milli amperes
Output Impedance	-	100 ohms
Input Impedance (SHORT & LONG Time Constant)	-	10^{11} ohms; 10^{14} ohms.
Frequency Response (nominal)	-	dc to 150000 cps
Linearity Error	-	0.1%
Noise (at output, with short cables)	-	1 milli volt
Input and output connectors	-	BNC coaxial
Line Power	-	115 volts, 60 cps / 210 to 240 volts, 50 to 60 cps.

KISTLER INSTRUMENT CORPORATION (U.S.A)

5. Oscilloscope

a. Type - 502 A Dual - Beam Oscilloscope.

The Oscilloscope provides linear dual - beam displays with a wide range of sweep rates combined with high input sensitivity. It may be used to provide dual - beam X - Y displays medium sensitivities, and single - beam X - Y displays at high sensitivities. Vertical amplifiers for both beams may be operated with single - ended inputs for conventional operation, or with differential inputs for cancellation of common mode signals.

In the vertical deflection system, there are seventeen calibrated deflection factors from 0.1 mv/cm to 20 v/cm accurate within 3%.

In the Horizontal - deflection system, there are twenty-one calibrated sweep rates from 1 μsec/cm to 5 sec/cm.

b. Type - 564 Storage Oscilloscope

This is a special purpose oscilloscope designed to store cathode - ray tube displays for viewing or photographing up to an hour after application of the input signal. This can be operated as a conventional oscilloscope also.

There are two separate storage screens of the cathode-ray - tube. Either the upper or lower storage screen in storage mode can be used while the other screen can be operated in non - store.

The Plug in units used are :

1. Type 3A3 Amplifier Unit
2. Type 3B4 Time Base Plug-in Unit.

TEKTRONIX INC. BEAVERTON, OREGON, (U.S.A.)

CHAPTER III

THEORETICAL INVESTIGATION

3.1 General

The effect of ~~mass~~ blast load on structural elements can be studied as transient vibration problem, when the structural element is subjected to an impulse load.

The analysis has been carried out for plates without any holes. Basic assumptions are :

(1) A normal to the middle plane remains normal to the deformed middle surface and does not change in its length.

(2) Normal stresses transverse to the middle plane can be neglected.

(3) The middle plane of the plate is not strained (It is called a neutral plane).

(4) Strain - displacement relations are linear.

(5) Effect of shear force on deflection is neglected as its contribution to the latter is small as compared to bending.

(6) Damping has not been considered.

Equation of flexural vibration of plates is given by:

$$D \nabla^4 w + \rho h \frac{\partial^2 w}{\partial t^2} = f(x, y, t) \qquad (3.1.1)$$

Introducing the non - dimensional parameters,

$$w = W \left(\frac{1.a^4}{D} \right)$$

$$X = \frac{x}{a}$$

$$Y = \frac{y}{b}$$

$$T = t \sqrt{\frac{D}{\rho h a^4}}$$

$$R = \frac{a}{b}$$

Substituting them in equation (3.1.1) we get

$$D\left[\frac{\partial^4 w}{\partial x^4} + 2 \frac{\partial^4 w}{\partial x^2 \partial y^2} + \frac{\partial^4 w}{\partial y^4}\right] + \rho h \frac{\partial^2 w}{\partial t^2} = f(x, y, t)$$

or $$D\left[\frac{a^4}{D.a^4} \frac{\partial^4 W}{\partial X^4} + 2 \frac{a^4}{a^2 b^2 D} \frac{\partial^4 W}{\partial X^2 \partial Y^2} + \frac{a^4}{D.b^4} \frac{\partial^4 W}{\partial Y^4}\right]$$

$$+ \frac{\rho h.a^4}{D} \frac{D}{\rho h a^4} \frac{\partial^2 W}{\partial T^2} = f(X, Y, T)$$

where f (X, Y, T) is the forcing function in non-dimensionalised form.

or $$\frac{\partial^4 W}{\partial X^4} + 2 R^2 \frac{\partial^4 W}{\partial X^2 \partial Y^2} + R^4 \frac{\partial^4 W}{\partial Y^4} + \frac{\partial^2 W}{\partial T^2}$$

$$= f(X, Y, T) \qquad (3.1.2)$$

3.2 Method of Solution

The equation of motion for vibration of plate can be written as

$$L\left[W(P, t)\right] + M(P)\frac{\partial^2 W(P, t)}{\partial t^2} = f(P, t) + F_j(t)\,\delta(P - P_j) \qquad (3.2.1)$$

Where L is a linear homogeneous self - adjoint differential operator consisting of derivatives with respect to spatial co-ordinates but not with respect to time t. The operator L contains the information concerning the stiffness distribution. The mass distribution is given by M (P). The excitation consists of the distributed force f (P, t) and the concentrated forces of amplitude $F_j(t)$ and acting at points $P = P_j$. $\delta(P - P_j)$ indicates spatial Dirac's delta function defined by

$$\delta(P - P_j) = 0 \qquad P \neq P_j$$
$$\int_D \delta(P - P_j)\, dD(P) = 1 \qquad (3.2.2)$$

The p boundary conditions are of the type

$$B_i\left[W(P, t)\right] = 0, \qquad i = 1, 2, \ldots \qquad (3.2.3)$$

where B_i are linear homogeneous differential operators.

The solution of the special eigen value problem of the differential equation

$$L\left[W\right] = \omega^2 N\left[W\right]$$

to be satisfied over domain D, where W is subject to the boundary conditions

$$B_i\left[W\right] = 0 \qquad (3.2.4)$$

consists of an infinite set of denumerable eigen functions $W_r(P)$ with corresponding natural frequencies w_r. The eigen functions are orthogonal and if they are normalised such that

$$\int_D M(P)\, W_r(P)\, W_s(P)\, dD(P) = \delta_{rs} \qquad (3.2.5)$$

it follows that

$$\int_D W_r(P)\, L\left[W_s(P)\right]\, dD(P) = w_r^2\, \delta_{rs} \qquad (3.2.6)$$

Using the expansion theorem, we write the solution of (3.2.1) as a superposition of the normal modes $W_r(P)$ multiplying corresponding time - dependent generalised displacement co-ordinates $n_r(t)$. Hence

$$W(P, t) = \sum_{r=1}^{\infty} W_r(P)\; n_r(t) \qquad (3.2.7)$$

Introducing this into partial differential equation, we get

$$L\left[\sum_{r=1}^{\infty} W_r(P)\, n_r(t)\right] + M(P)\frac{\partial^2}{\partial t^2}\sum_{r=1}^{\infty} W_r(P)\, n_r(t)$$

$$= f(P, t) + F_j(t)\,\delta(P - P_j) \quad (3.2.8)$$

Multiplying both sides of (3.2.8) by $W_s(P)$ and integrating over the domain D,

$$\sum_{r=1}^{\infty} n_r(t)\int_D W_s(P)\, L\left[W_r(P)\right] dD(P) +$$

$$\sum_{r=1}^{\infty} \ddot{n}_r(t)\int_D W_s(P) M(P) W_r(P)\, dD(P)$$

$$= \int_D W_s(P)\,(f(P, t) + F_j(t)\,\delta(P - P_j))\, dD(P) \quad (3.2.9)$$

In view of (3.2.5) and (3.2.6)

$$\ddot{n}_r(t) + w_r^2\, n_r(t) = N_r(t) \qquad r = 1, 2, \ldots \quad (3.2.10)$$

where

$$N_r(t) = \int_D W_r(P)\, f(P, t)\, dD(P) + \sum_{j=1}^{1} W_r(P_j) F_j(t) \quad (3.2.11)$$

and denotes a generalised force associated with the generalised co-ordinate $n_r(t)$.

Equation (3.2.10) represents an infinite set of uncoupled ordinary differential equations similar to the single degree of freedom system equation.

Applying Laplace transform technique, equation (3.2.10) reduces to

$$s^2 \bar{n}_r(s) - s\, n_r(0) - \dot{n}_r(0) + w_r^2 \bar{n}_r(s) = \bar{N}_r(s) \qquad (3.2.12)$$

or,

$$\bar{n}_r(s) = \frac{s\, n_r(0)}{s^2 + w_r^2} + \frac{\dot{n}_r(0)}{s^2 + w_r^2} + \frac{\bar{N}_r(s)}{s^2 + w^2} \qquad (3.2.13)$$

Taking the inverse transform, we get

$$n_r(t) = \frac{1}{w_r} \int_0^t N_r(\tau) \sin w_r(t - \tau)\, d\tau + n_r(0) \cos w_r t + \dot{n}_r(0) \frac{\sin w_r t}{w_r} \qquad (3.2.14)$$

where $n_r(0)$ and $\dot{n}_r(0)$ are the initial generalised displacement and initial generalised velocity given by

$$n_r(0) = \int_D M(P)\, W_r(P)\, W(P,0)\, dD(P)$$

$$\dot{n}_r(0) = \int_D M(P)\, W_r(P)\, \dot{W}(P,0)\, dD(P) \qquad r = 1,2.. \qquad (3.2.15)$$

3.3 Assumed Mode Method

It is not always possible to know exact solution for the mode shape of a continuous system for different boundary conditions. The response of a continuous system is then assumed to be in the form

$$W_r (P, t) = \sum_{i=1}^{n} W_i (P)\, q_i (t) \qquad (3.3.1)$$

where W_i (P) are admissible functions, which are functions of the spatial co-ordinates P, and satisfy the geometric boundary conditions of the system, and q_i (t) are time - dependent generalised displacement co-ordinates. In this manner a continuous system is approximated by an n - degree of freedom system. The kinetic energy of the system is

$$T (t) = \tfrac{1}{2} \sum_{i=1}^{n} \sum_{j=1}^{n} m_{ij}\, \dot{q}_i (t)\, \dot{q}_j (t) \qquad (3.3.2)$$

where the mass co-efficients depend on mass distribution M (P) and the admissible functions W_i (P). The potential energy can be written

$$V (t) = \tfrac{1}{2} \sum_{i=1}^{n} \sum_{j=1}^{n} K_{ij}\, q_i (t)\, q_j (t) \qquad (3.3.3)$$

where the stiffness co-efficients depend on the stiffness properties of the system and the admissible functions W_i (P) and its derivatives.

If any non-conservative forces are present, Lagrange's equations of motion have the form

$$\frac{d}{dt} \left(\frac{\partial T}{\partial \dot{q}_r} \right) - \frac{\partial T}{\partial q_r} + \frac{\partial V}{\partial q_r} = Q_r \qquad r = 1, 2 \ldots \qquad (3.3.4)$$

where $Q_r(t)$ are time - dependent non-conservative generalised forces and are given by

$$Q_r(t) = \int_D f(P, t)\, W_r(D)\, dD(P) + \sum_{j=1}^{l} F_j(t)\, W_r(P_j) \quad ; \; r = 1,2, \ldots n \qquad (3.3.5)$$

and l is the number of concentrated forces. Lagrange's equation of motion become

$$\sum_{j=1}^{n} m_{rj}\, \ddot{q}_j(t) + \sum_{j=1}^{n} K_{rj}\, q_j(t) = Q_r(t) \qquad r = 1,2..n \qquad (3.3.6)$$

And in the matrix form

$$[m]\{\ddot{q}(t)\} + [K]\{q(t)\} = \{Q(t)\} \qquad (3.3.7)$$

This method has been used to calculate the natural frequency and response of the clamped plate.

3.4 Simply Supported Plates

In case of simply supported plates, the eigen functions are known and therefore the method discussed in section 3.2 can be used.

The mode shapes are given as

$$W_{mn}(X, Y) = A_{mn} \sin(m\pi X) \sin(n\pi Y) \qquad (3.4.1)$$

$$L = \frac{\partial^4 W}{\partial X^4} + 2R^2 \frac{\partial^4 W}{\partial X^2 \partial Y^2} + R^4 \frac{\partial^4 W}{\partial Y^4}$$

$$M = 1$$

The boundary conditions are

$$W(0, Y) = W(1, Y) = W(X, 0) = W(X, 1) = 0$$

$$\frac{\partial^2 W}{\partial X^2}(0, Y) = \frac{\partial^2 W}{\partial X^2}(1, Y) = \frac{\partial^2 W}{\partial Y^2}(X, 0) = \frac{\partial^2 W}{\partial Y^2}(X,1) =$$

The eigen functions are orthogonal and normalising, we get

$$\int_0^1 \int_0^1 M(X, Y)\, W_{mn}(X, Y)\, W_{rs}(X, Y)\, dX\, dY = \delta_{mr}\delta_{ns}$$

or, $$\int_0^1 \int_0^1 (A_{mn})(A_{rs}) \sin(m\pi X) \sin(n\pi Y)$$

$$(\sin r\pi X)(\sin s\pi Y)\, dX\, dY = \delta_{mr}\delta_{ns}$$

$$\frac{(A_{mn})^2}{4} = 1$$

$$A_{mn} = 2 \qquad (3.4.2)$$

Now from (3.2.4)

$$\int_0^1 \int_0^1 W_{rs}(P)\, L\left[W_{mn}(P)\right] dD(P) = w_{mn}^2 \delta_{mr}\delta_{ns}$$

Substituting $W_{rs}(P)$ and $W_{mn}(P)$, we get

$$\int_0^1 \int_0^1 \left[\frac{\partial^4}{\partial X^4} + 2R^2 \frac{\partial^4}{\partial X^2 \partial Y^2} + R^4 \frac{\partial^4}{\partial Y^4}\right](W_{mn}(X,Y))$$

$$W_{rs}(X, Y)\, dX\, dY = w_{mn}^2 \delta_{mr}\, \delta_{ns}$$

$$\int_0^1 \int_0^1 4\left((m\pi)^4 + 2R^2 (m\pi)^2 (n\pi)^2 + (R^4)(n\pi)^4\right)$$

$$\sin m\pi X \cdot \sin n\pi Y \cdot \sin r\pi X \cdot \sin s\pi Y \, dX \, dY$$

$$= \bar{w}_{mn}^2 \delta_{mr} \delta_{ns}$$

$$\bar{w}_{mn}^2 = \pi^4 \left(m^4 + 2R^2 m^2 n^2 + R^4 n^4 \right)$$

$$= \pi^4 (m^2 + R^2 n^2)^2$$

$$\bar{w}_{mn} = \pi^2 (m^2 + R^2 n^2) \qquad (3.4.3)$$

where $\bar{w}_{mn}$ is the non - dimensionalised natural frequency.

The natural frequency is given by

$$w_{mn} = \pi^2 \sqrt{\frac{D}{\rho h a^4}} \, (m^2 + R^2 n^2) \qquad (3.4.4)$$

$$= \sqrt{\frac{D}{\rho h a^4}} \; \bar{w}_{mn}$$

From (3.2.7)

$$W(X, Y, T) = \sum_{m=1}^{\infty} \sum_{n=1}^{\infty} 2 \sin m\pi X \cdot \sin n\pi Y \; n_{mn}(T) \qquad (3.4.5)$$

Substituting this in equation (3.1.2), multiplying by $\sin r\pi X \cdot \sin s\pi Y$ and integrating over the region (0, 1), (0, 1), we get

$$\pi^4 (m^2 + R^2 n^2)^2 n_{mn}(T) + \ddot{n}_{mn}(T)$$

$$= \int_0^1 \int_0^1 2 f(X, Y, T) \sin m\pi X \cdot \sin n\pi Y \cdot dX\, dY$$

$$f(X,Y,T) = f(T)$$

or,

$$\ddot{n}_{mn}(T) + \bar{w}_{mn}^2 n_{mn}(T) = \frac{8}{mn\pi^2} f(T) \qquad (3.4.6)$$

when both m and n are odd

$$= 0 \quad \text{otherwise}$$

From (3.2.14)

$$n_{mn}(T) = \frac{1}{\bar{w}_{mn}} \int_0^T \frac{8}{mn\pi^2} f(\tau) \sin \bar{w}_{mn}(T-\tau)\, d\tau$$

$$+ n_{mn}(0) \cos \bar{w}_{mn} T + \dot{n}_{mn}(0) \frac{\sin \bar{w}_{mn} T}{\bar{w}_{mn}} \qquad (3.4.7)$$

In our case,

$$n_{mn}(0) = 0$$

$$\dot{n}_{mn}(0) = 0 \qquad (3.4.8)$$

$$n_{mn}(T) = \frac{1}{\bar{w}_{mn}} \int_0^T \frac{8}{mn\pi^2} f(\tau) \sin \bar{w}_{mn}(T-\tau)\, d\tau \qquad (3.4.9)$$

The integral $\int_0^T f(\tau) \sin \bar{w}_{mn}(T-\tau)\, d\tau$ is called the "Response function" (or Duhamel Integral) and is dependent upon the type of forcing function used. It

has been calculated for different types of pulse loading. and given in Appendix A.

Substituting $n_{mn}(T)$ in (3.4.5), we have

$$W(X, Y, T) = \sum_{m=1,3}^{\infty} \sum_{n=1,3}^{\infty} \frac{8 W_{mn}(X, Y)}{mn\pi^2 \bar{w}_{mn}} \int_0^T f(\tau) \sin \bar{w}_{mn}(T - \tau)\, d\tau \qquad (3.4.10)$$

The strains in terms of non - dimensionalised parameters in X and Y directions are given by.

$$\bar{e}_x = -\frac{\partial^2 W}{\partial X^2} = \text{strain in x - direction}$$

and;

$$\bar{e}_y = -\frac{\partial^2 W}{\partial Y^2} = \text{strain in y - direction}$$

$$\bar{e}_x = \sum_{m=1,3}^{\infty} \sum_{n=1,3}^{\infty} \frac{16m}{n \bar{w}_{mn}} \sin m\pi X \sin n\pi Y \int_0^T f(\tau) \sin \bar{w}_{mn}(T - \tau)\, d\tau \qquad (3.4.11)$$

and

$$\bar{e}_y = \sum_{m=1,3}^{\infty} \sum_{n=1,3}^{\infty} \frac{16n}{m \bar{w}_{mn}} \sin m\pi X \cdot \sin n\pi Y \int_0^T f(\tau) \sin \bar{w}_{mn}(T - \tau)\, d\tau \qquad (3.4.12)$$

The actual strains are given by

$$e_x = \frac{h}{2} \frac{a^2}{D} \bar{e}_x$$

$$= \frac{h}{2} \frac{a^2}{D} \sum_{m=1,3}^{\infty} \sum_{n=1,3}^{\infty} \frac{16\,m}{n\,\bar{w}_{mn}} \sin m\pi X \cdot \sin n\pi Y \int_0^T f(\tau) \sin \bar{w}_{mn} (T - \tau)\, d\tau \qquad (3.4.11a)$$

and

$$e_y = \frac{h}{2} \frac{a^2}{D} R^2 \bar{e}_y$$

$$= \frac{h}{2} \frac{a^2}{D} R^2 \sum_{m=1,3}^{\infty} \sum_{n=1,3}^{\infty} \frac{16\,n}{m\,\bar{w}_{mn}} \sin m\pi X \cdot \sin n\pi Y \int_0^T f(\tau) \sin \bar{w}_{mn} (T - \tau)\, d\tau \qquad (3.4.12a)$$

3.5 Clamped Plates

In the case of clamped plates it is not possible to give an exact solution for the mode shape of the plate. However, a good approximation is given by the product of the expressions for a clamped beam.

$$W_{mn}(X, Y) = W_m(X) \cdot W_n(Y) \qquad (3.5.1)$$

where

$$W_m(X) = \bar{W}_m(X) \Big/ \left|\bar{W}_m(X)\right|$$

$$W_n(Y) = \bar{W}_n(Y) \Big/ \left|\bar{W}_n(Y)\right| \qquad (3.5.2)$$

where,

$$\bar{W}_m(X) = (A_m - 1) \sinh \alpha_m X + A_m \left[\exp(-\alpha_m X) - \cos \alpha_m X\right] + \sin \alpha_m X \qquad (3.5.3)$$

$$\bar{W}_n(Y) = (A_n - 1) \sinh \alpha_n Y + A_n \left[\exp(-\alpha_n Y) - \cos \alpha_n Y\right] + \sin \alpha_n Y$$

$$\cos \alpha \cosh \alpha = 1 \qquad (3.5.7)$$

$$\alpha_1 = 4.73004, \quad \alpha_2 = 7.85320$$

$$\alpha_n = \frac{2n+1}{2} \qquad n > 2 \qquad (3.5.7a)$$

$$\psi_m = \alpha_m^2 \left[\tfrac{1}{2} \left(\frac{1}{\cos^2 \frac{\alpha_m}{2}} - \frac{1}{\cosh^2 \frac{\alpha_m}{2}} \right) - \frac{2}{\alpha_m} \tanh \frac{\alpha_m}{2} \right] \qquad (3.5.8)$$

let

$$W(X, Y, T) = \sum_{m=1}^{\infty} \sum_{n=1}^{\infty} W_m(X)\, W_n(Y)\, n_{mn}(T) \qquad (3.5.9)$$

Substituting this in equation (3.1.2), multiplying by $W_{rs}(X, Y)$ and integrating over the region (0, 1), (0, 1), we get

$$\ddot{n}_{mn}(T) + \bar{w}_{mn}^2 \, n_{mn}(T) = \frac{1}{M_{mn}} \int_0^1 \int_0^1 W_{mn}(X, Y)$$

$$f(X, Y, T)\, dX\, dY$$

where M_{mn} is the generalised mass given by

$$M_{mn} \int_0^1 \int_0^1 \left(W_{mn}(X, Y) \right)^2 dX\, dY = M_m\, M_n \qquad (3.5.10)$$

where

$$M_m = \int_0^1 \left(W_m(X) \right)^2 dX$$

&

$$M_n = \int_0^1 \left(W_n(Y) \right)^2 dY \qquad (3.5.11)$$

For our case,

$$F(X, Y, T) = F(T)$$

Therefore, we get

$$\ddot{n}_{mn}(T) + \bar{w}_{mn}^2 n_{mn}(T) = \frac{1}{M_{mn}} \int_0^1 \int_0^1 W_m(X)\, W_n(Y)$$

$$f(T)\, dX\, dY$$

Substituting the values of $W_m(X)$, $W_n(Y)$ and integrating, we get

$$\ddot{n}_{mn}(T) + \bar{w}_{mn}^2 n_{mn}(T) = \frac{1}{\alpha_m \alpha_n M_{mn}} \bar{Q}_m \bar{Q}_n f(T) \qquad (3.5.12)$$

where

$$\bar{Q}_m = \left[(A_m - 1) \cosh \alpha_m - A_m (\exp(-\alpha_m) + \sin \alpha_m) + 2 - \cos \alpha_m \right] / \left| \bar{W}_m(X) \right| \qquad (3.5.13)$$

$$\bar{Q}_n = \left[(A_n - 1) \cosh \alpha_n - A_n (\exp(-\alpha_n) + \sin \alpha_n) + 2 - \cos \alpha_n \right] / \left| \bar{W}_n(Y) \right|$$

Assuming initial conditions to be zero, we have

$$n_{mn}(T) = \frac{\bar{Q}_m \bar{Q}_n}{\alpha_m \alpha_n M_m M_n \bar{w}_{mn}} \int_0^T f(\tau) \sin \bar{w}_{mn} (T - \tau) d\tau \qquad (3.5.14)$$

$$W(X, Y, T) = \sum_{m=1}^{\infty} \sum_{n=1}^{\infty} \frac{\bar{Q}_m \cdot \bar{Q}_n W_m(X) W_n(Y)}{\alpha_m \alpha_n M_m M_n \bar{w}_{mn}} \int_0^T f(\tau) \sin \bar{w}_{mn} (T - \tau)\, d\tau \qquad (3.5.15)$$

Strains in non-dimensionalised parameters in x and y directions are respectively (at $Z = h/2$)

$$\bar{e}_x = -\frac{\partial^2 W}{\partial X^2}$$

$$= -\sum_{m=1}^{\infty}\sum_{n=1}^{\infty}\frac{\alpha_m \bar{Q}_m \bar{Q}_n}{\alpha_n M_m M_n \bar{w}_{mn}} \bar{P}_m(X)\, W_n(Y)$$

$$\int_0^T f(\tau)\sin \bar{w}_{mn}(T-\tau)\, d\tau \qquad (3.5.16)$$

and

$$\bar{e}_y = -\sum_{m=1}^{\infty}\sum_{n=1}^{\infty}\frac{\alpha_n \bar{Q}_m \bar{Q}_n}{\alpha_m M_m M_n \bar{w}_{mn}} W_m(X)\, \bar{P}_n(Y)$$

$$\int_0^T f(\tau)\sin \bar{w}_{mn}(T-\tau)\, d\tau \qquad (3.5.17)$$

where

$$\bar{P}_m(X) = ((A_m - 1)\sinh \alpha_m X + A_m \exp(-\alpha_m X) + \cos \alpha_m X) - \sin \alpha_m X) / |\bar{W}_m| \qquad (3.5.18)$$

$$\bar{P}_n(Y) = ((A_n - 1)\sinh \alpha_n Y + A_n \exp(-\alpha_n Y) + \cos \alpha_n Y) - \sin \alpha_n Y) / |\bar{W}_n|$$

The actual strains are given by

$$e_x = \frac{h}{2}\frac{a^2}{D}\bar{e}_x \qquad (3.5.16a)$$

$$e_y = \frac{h}{2}\frac{a^2}{D}\bar{e}_y R^2 \qquad (3.5.17a)$$

CHAPTER IV

RESULTS AND DISCUSSIONS

4.1 Theoretical Results

The response of a plate to impulsive loading has been computed. The computer program gives the strains and displacements at any point on the plate as a function of time and it also gives the modal contributions. In the case considered ($b > a$) it is found that the contribution of higher modes is less for deflection and strain in x - direction, e_x. But the contribution of higher modes for strain in y direction, e_y, is larger.

The convergence was very good for simply supported plates considering six harmonics. For clamped plates nine harmonics were used and the convergence was satisfactory.

In Table 1b, the values of the deflection at the center for clamped plates and simply - supported plates have been compared. The values are given for the impulse of unit magnitude. The non-dimensionalised deflections are also given for static case.

4.2 Experimental Results

The experiment has been carried out for clamped plates for a constant aspect ratio (b/a) and varying thickness h. The values of pressure and strains are given in Tables.

4.3 Graphical Plots

Figure 7 is the calibration curve for rosettes and strain gauges. The static calibration of the pressure transducer was done and it agreed satisfactorily with the calibration constant given by the manufacturer. Fig. 8 shows the actual pressure acting on the plate for different pressures in high pressure chamber. Figures 9a and 9b show respectively the pressure curves when there is an opening in the plate and when there is no opening.

In figures 11.a to 11.c, the pressure acting on the plate has been plotted against ratio of hole area to plate area for different types of holes. For ratio 1 (i.e. there is no plate at all), the pressure transducer was kept at the end section of the shock - tube.

The response of the plates to blast load has been given in terms of strains. Strains are given

for the center of the clamped edges in both the directions. Figures 14 to 16 show the variation of e_x with different area ratios when the thickness and pressure are kept constant The values are plotted for different pressures. Similarly the variation of strain in y direction with different area ratios for a particular thickness keeping the pressure constant is shown in figures 17 to 19.

To see the effect of thickness on the response for a particular area ratio, graphs have been drawn between strains and the ratio of thickness to plate length in x - direction.

4.4 Discussion

The values of strains at the ends and at the center of a plate without a hole are compared with the theoretical results. The experimental and theoretical values are in good agreement for plates 2 and 3. For plate 1, the experimental values are considerably less than the theoretical values. This may be because of the fact that for large deflections, membrane forces come into play and have to be taken into consideration in the analysis. It is found that the Dynamic Amplification Factor,(defined as the ratio of dynamic strains (or moments) to static strains (or moments) when the

peak dynamic load is assumed to be uniformly distributed on the plate) at the ends is much less than at the center. The ratio is 3 to 4 times at the ends where as it is less than 2 for the strains at the ends.

The theoretical values of deflection for the clamped - clamped plate and simply supported plate for the experimental pulse shape is compared with the static deflection assuming the peak dynamic pressure to be uniformly acting on the plate. It is observed that for the pulse shape considered the ratio of dynamic deflection to static deflection is less in clamped plates than in simply supported plates.

Figures 13 to 18 give response of the plate with and without holes. It is seen that for all plates e_x increases for holes of shapes 1 and 3 at lower area - ratios. At area - ratios around 1/16, the strains increase considerably for shapes 2 and 3 but decrease for shape 1. The strains for ratios 1/4 are minimum for plates with holes of shape 2 in all the cases. This is due to the fact that the bending strain at the hole in a direction perpendicular to it has to be zero. (In this case the gages are located considerably near the holes). Also the total

force acting at the point where the gage is fixed is less for plates with holes of shape 2 than for plates with holes 1 and 3.

Figures 16 to 19 represent the response in terms of dynamic strains in y directions (or moments). It is found that e_y first decreases with increase in area ratios. But for the maximum area ratio, e_y increase appreciably for holes of shape 2. In other shapes also, there is an increase, but it is very less as compared to the hole of shape 2.

In general, there are two effects of holes on the response of plates. In the first, the total stiffness of the plate is reduced. At the same time, when the load is uniformly distributed, the total load is smaller in the case of a plate with the holes. When a central cut out is made, for the same intensity of the distributed load, a smaller total load acts on a relatively stiffer portion. Thus one expects a smaller maximum deflection when a central cut-out is made.

In case of strains an additional parameter is the distance of the gage location from the nearest free edge of the hole. Farther it is from the hole, the larger is the strain. The nature of variation of

strains as a function of areas of holes, is then due to the combined effect of the above mentioned factors.

In light of the above factors, figures 13 to 18, where the strains are plotted as a function of the relative areas of the holes, with the shape of the hole as a parameter are drawn, can be interpreted.

In case of circular holes, the graphs drawn for e_y and e_x reveal different trends. At higher values of hole ratios, e_y (at the center of clamped edge parallel to x axis) increases whereas e_x decreases. It seems that e_y is influenced more by the reduction in total stiffness than by the presence of a free edge which is farther removed from the gage location as compared to the gage location for e_x. For smaller holes one expects that the change in the values of the strains as compared to solid plates to be little and this is clear from the graphs.

CHAPTER - V

CONCLUSIONS AND SCOPE FOR FURTHER WORK

5.1 Conclusions

The theory discussed in Chapter III assumes the deflection to be small. The initial strains in clamped plates is not considered in the theory. Graphs have been given to show the effect of holes in the response of plates (clamped) and the variation in pressure distribution due to these holes. The following conclusions are drawn :

1. The dynamic amplification factor for moments (or strains) is more at the center than at the ends for clamped plates.

2. The computed values of dynamic amplification factor in clamped plates are less than those for simply supported plates.

3. With increase in area - ratios, the strains at the ends along the line parallel to longer edge decrease. But as the area - ratio increases, the strains increase. Whereas for larger area - ratios, the strains at the ends along the line parallel to shorter edge decrease.

4. The pressure drops with increase in area ratios. The drop rate increases with increase in area - ratios.

5. To be of assistance in designing against internal explosions the following observations are made:

Cut-outs help in reducing the overpressures acting on the structure. Although other considerations may influence the choice, regarding the shape and size, where ever possible larger areas of cut-outs are to be preferred.from the point of reducing the intensity.

For the same area of openings, those with the larger side parallel to the larger edge of the plate are preferable to those with longer sides parallel to shorter edges. Where ever possible, circular openings should also be considered as they are definitely better than those of the latter described above, and may compare favourably with the former type described above.

5.2 Scope For Further Work :

Experiments on similar lines can be conducted on plates with several holes so as to be of guidance while designing.

Brittle coating technique may be contemplated to obtain a complete knowledge of the strain field.

Instrumentation techniques to measure dynamic deflections and over pressures are to be developed.

The shock tube can be readily used to conduct blast loading on various structural elements and for different end conditions and can be modified without difficulty to obtain partial loading also on these elements.

Finite element method may be used for plates with cut-outs to predict the response based on theory.

REFERENCES

1. FRANKLAND, J.M. - "Effect of Impact on Simple Elastic Structures", Proceedings of the Society for Experimental Stress Analysis, Vol. VI, No.2 pp. 7 - 27.

2. CHENG, D.H. and BENVENISTE, J.E. - "Response of Structural Elements to Travelling Pressure Waves of Arbitrary Shape", Internal Journal of Mechanical Sciences, 8, pp 607 - 618, 1966.

3. BAKER, W.E., EWING, W.O and Others - "The Elastic and Plastic Response of Cantilevers to Air Blast Loading". Proc. IV U.S. National Congress of Applied Mechanics, ASME, Vol. 2, pp. 853 - 866, 1962.

4. BANERJEE, S.K. - "Dynamic Response of Beams to Blast Load" M.Tech. Thesis, I.I.T. Kanpur, Kanpur - 16, 1971.

5. SYMONDS, P.S. and BODNER, S.R. - "Experimental and Theoretical Investigation of the Plastic Deformation of Cantilever Beams Subjected to Impulsive Loading", Journal of Applied Mechanics, Vol. 29, Trans. ASME, Vol. 82, p. 719, 1962.

6. TING, T.C.T. - "The Plastic Deformation of a Cantilever Beam with Strain - Rate Sensitivity Under Impulsive Loading", Journal of Applied Mechanics, Vol. 31, pp. 38 - 42, March. 1964.

7. MARTIN, J.B. and LEE, L.S.S. - "Approximate Solutions for Impulsively Loaded Elastic - Plastic Beams", Presented at the Winter Annual Meeting. New York, December 1 - 5, 1968 of the ASME.

8. GEORGE, P.J. - "Dynamic Response of Circular Plates to Pulse Loads". Presented at the 23rd Annual General Meeting Aeronautical Society of India held at I.I.T. Kanpur, Feb. 26 - 28, 1971.

9. WANG, A.J. - "The Permanent Deflection of a Plastic Plate under Blast Loading" - Journal of Applied Mechanics, Vol. 22, pp. 375 - 376, Sept. 1955.

10. GLASSTONE, S. - "The Effects of Nuclear Weapons". Prepared by U.S. Department of Defence and Published by U.S. Atomic Energy Commission, April, 1962.

11. CARLSON, H.W., MACK, R.J. and MORRIS, O.A. - "Sonic Boom Pressure - Field Estimation Techniques". Journal of Acoustical Society of America, 39, No. 5, pt. - 2, 1966, Sonic Boom Symposium pp - 510 - 518.

12. FLORENCE, A.L. - "Circular Plates Under Uniformly Distributed Impulse". International Journal of Solids and Structures, 2, pp. 37 - 47, 1966.

13. NORMAN JONES, - URAN, T.O. and TEKIN, S.A. "The Dynamic Plastic Behaviour of Fully Clamped Rectangular Plates" International Journal of Solids and Structures, Vol. 6, pp. 1499-1512, 1970.

14. NORMAL JONES - "A Theoretical Study of The Dynamic Plastic Behaviour of Beams". International J. Solids Structures, Vol. 7, pp. 1007 - 1029,1971.

15. YOUNGDAHL, C.K. - "Influence of Pulse Shape on The Final Plastic Deformation of a Circular Plate". International J. Solids Structures, Vol. 7, pp. 1127 - 1142, 1971.

16. ALLGOOD, J.R. and SWIHART, G.R. - "Design of Flexural Members for Static and Blast Loading". American Concrete Institute.

17. HAMBLEY, E.C. - "Discussion on Explosions in Domestic Structures". The Structural Engineer, Vol. 47, No. 10, pp. 319 - 329, October, 1969.

18. RASBASH, D.J. and STRETCH, K.L. - "Explosions in Domestic Structures". The Structural Engineer, Vol. 47, No. 10, pp. 403-411. October 1969.

27. WIGGINS, J.H. Jr. and KENNEDY, B. - "Theoretical Study of Structural Response to Near-Field and Far - Field Sonic Booms". Final Report Cont. No. AF 49 (638) - 1777 Data Craft. Inc. 1966.

28. LOWERY, R.L. and ANDREWS, D.K. - "Acoustical and Vibrational Studies Relating to An Occurrence of Sonic Boom Induced Damage to a Window Glass In a Store Front." NASA CR-66170, 1966.

29. LAUSING, D.L. and MAGLIERI, D.J. - "Comparison of Measured and Calculated Sonic - Boom Ground Patterns Due to Several Different Aircraft Maneuvers". NASA TN - D - 2730, 1965.

30. CROCKER, M.J. and HUDSON, P.R. - "Structural Responses to Sonic Booms". Journal of Sound and Vibration, Vol. 9, pp. 454 - 469, 1969.

31. SUI LIN - "Sonic Boom Analog for Investigatin Indoor Acoustical Waves". Journal of Acoustical Society of America, Vol. 49, No. 5 (Part 1), pp. 1386-1389, 1971.

32. THOMSON, R.G. - "Plastic Behaviour of Circular Plates Under Transverse Impulse Loading of Gaussian Distribution". NASA - TR - R - 279, January, 1968.

33. MEIROVITCH, L. "Analytical Methods in Vibration", Macmillan Company, New York, 1967

34. TIMOSHENKO, S. and WOINOWSKY, K.S. - "Theory of Plates and Shells" McGraw Hill Book Company, Inc.

35. HARRIS, C.M. and CREDE, C.E. - "Shock and Vibration Handbook". Volume 1, McGraw Hill Book Company.

36. DOVE R.C. and ADAMS P.H. - "Experimental Stress Analysis and Motion Measurement", Prentice - Hall of India Ltd. New Delhi, 1965.

37. NOWACKI WITOLD - "Dynamics of Elastic Systems" John Wiley and Sons. Inc., New York, 1963.

APPENDIX - A

RESPONSE FUNCTIONS

$$\text{Response function} = F.R(t) = \int_0^t f(\tau)\ \text{Sin w}\ \text{Sin } w(t-\tau)\, d\tau$$

1. Rectangular Pulse

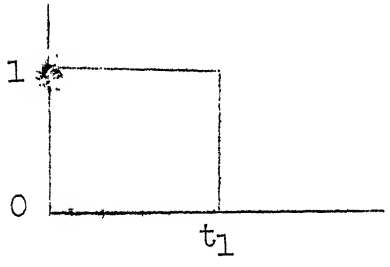

Forcing function :

$f(t) = 1$ for $t < t_1$

$= 0$ for $-\infty < t < 0$ and $t > t_1$

Response Function :

For $t < t_1$

$$F.R.(t) = \frac{1}{w}(1 - \cos w t)$$

For $t > t_1$

$$F.R(t) = \frac{1}{w}\left(\cos w(t - t_1) - \cos wt\right)$$

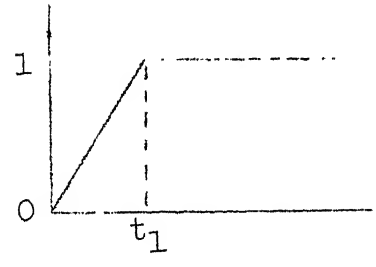

Forcing Function :

$f(t) = 0$, $-\infty < t < 0$

$= \frac{t}{t_1}$, $t < t_1$

$= 1$ $t \geq t_1$

Response function: For $t < t_1$

$$F.R.(t) = \frac{1}{wt_1}\left(t - \frac{\sin wt}{w}\right)$$

For $t > t_1$

$$F.R.(t) = \frac{1}{wt_1}\left[t_1 + \frac{\text{Sin } w(t - t_1)}{w} - \frac{\text{Sin } wt}{w}\right]$$

2. Triangular Pulse

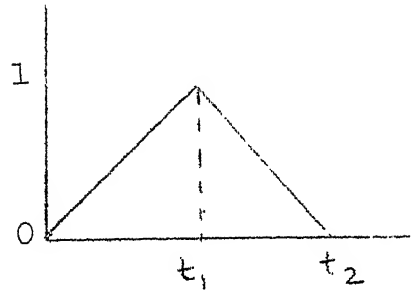

Forcing Function

$$f(t) = 0 \quad , -\infty < t < 0 \text{ and } t > t_2$$

$$= \frac{t}{t_1} \quad , \quad 0 < t < t_1$$

$$= 1 - \frac{t - t_1}{t_2 - t_1} \quad , \quad t_1 < t < t_2$$

Response Function

For $t < t_1$

$$\text{F.R. } (t) = \frac{1}{wt_1}\left(t - \frac{\text{Sin } wt}{w}\right)$$

For $t_1 < t < t_2$

$$\text{F.R. } (t) = \frac{1}{w}\left[1 - \frac{t-t_1}{t_2-t_1} - \frac{\text{Sin } wt}{wt_1} + \frac{\text{Sin } w(t-t_1)}{wt_1} + \frac{\text{Sin } w(t-t_1)}{w(t_2 - t_1)}\right]$$

and $t > t_2$

$$\text{F.R. } (t) = \frac{1}{w^2}\left[\frac{\text{Sin } w(t-t_1)}{t_1} + \frac{\text{Sin } w(t-t_1)}{t_2 - t_1} - \frac{\text{Sin } wt}{t_1} - \frac{\text{Sin } w(t - t_2)}{t_2 - t_1}\right]$$

3. Trapezoidal Pulse

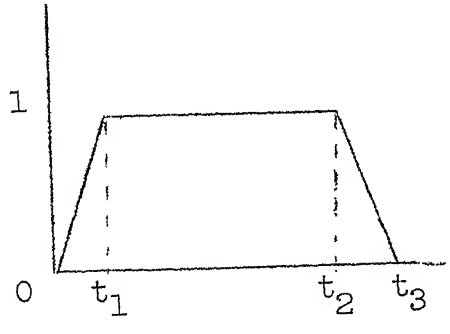

Forcing Function :

$$f(t) = 0 \quad , \quad -\infty < t < 0, \quad t > t_3$$

$$= \frac{t}{t_1} \qquad t < t_1$$

$$= 1 \qquad t_1 < t < t_2$$

$$= 1 - \frac{t-t_2}{t_3-t_2} \qquad t_2 < t < t_3$$

Response Function

For $t < t_1$

$$F.R.(t) = \frac{1}{w\,t_1}\left(t - \frac{\sin wt}{w}\right)$$

$t_1 < t < t_2$

$$F.R.(t) = \frac{1}{w\,t_1}\left[t_1 + \frac{\sin w(t-t_1)}{w} - \frac{\sin wt}{w}\right]$$

$t_2 < t < t_3$

$$F.R.(t) = \frac{1}{w^2 t_1}\left[w\,t_1 + \sin w(t-t_1) - \sin wt\right] - \frac{1}{w^2(t_3-t_2)}\left(w(t-t_2) - \sin w(t-t_2)\right)$$

$t > t_3$

$$.R.(t) = \frac{1}{w}\left[\frac{\sin w(t-t_1)}{w\,t_1} - \frac{\sin wt}{w\,t_1} - \frac{\sin w(t-t_3)}{w(t_3-t_2)} + \frac{\sin w(t-t_2)}{w(t_3-t_2)}\right]$$

4. Trapezoidal Pulse with Zero Rise Time

Forcing Function

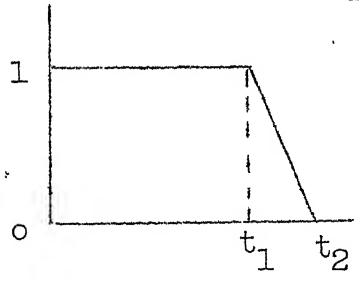

$$f(t) = 0 \quad , -\infty < t < 0 \;\&\; t > t_2$$

$$= 1 \quad , \quad t < t_1$$

$$= 1 - \frac{t-t_1}{t_2-t_1} \quad , \quad t_1 < t < t_2$$

Response Function

For $t < t_1$

$$FR(t) = \frac{1}{w}(1 - \cos wt)$$

$t_1 < t < t_2$

$$F.R.(t) = \frac{1}{w}\left[1 - \frac{t-t_1}{(t_2-t_1)} - \cos wt + \frac{1}{w(t_2-t_1)} \sin w(t - t_1)\right]$$

$t > t_2$

$$F.R.(t) = -\frac{\cos wt}{w} - \frac{\text{Sin } w(t-t_2)}{w^2(t_2-t_1)} + \frac{1}{w^2(t_2-t_1)} \sin w(t - t_1)$$

5.

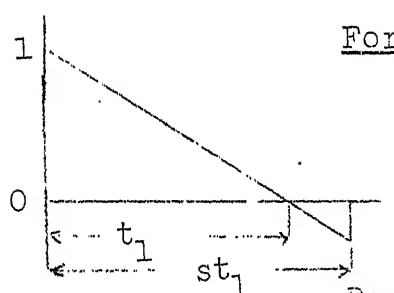

Forcing Function

$$f(t) = 0 \quad , \quad -\infty < t < 0 \;\&\; t > s t_1$$

$$= 1 - \frac{t}{t_1} \quad , \quad 0 < t < s t_1$$

Response Function

$t < st_1$

$$FR(t) = \frac{1}{w}\left(1 - \frac{t}{t_1} - \cos wt + \frac{\text{Sin } wt}{wt_1}\right)$$

$t > st_1$

$$FR(t) = \frac{(1-s)}{w} \cos w(t - s t_1) - \frac{1}{w^2 t_1} \text{Sin } w(t - s t_1) + \frac{\text{Sin } wt}{w^2 t_1} - \frac{\cos wt}{w}$$

This is a special case of the previous one with

$S = 1$

Response Function

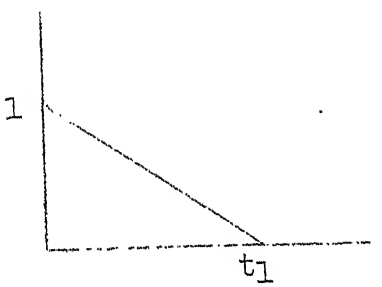

for $t < t_1$

$$FR(t) = \frac{1}{w}\left[1 - \frac{t}{t_1} - \cos wt + \frac{\sin wt}{w\, t_1}\right]$$

for $t > t_1$

$$FR(t) = \frac{1}{w}\left[-\frac{\sin w(t - t_1)}{w\, t_1} - \cos wt + \frac{\sin wt}{wt_1}\right]$$

APPENDIX - B

The static response of simply supported plates has been obtained from Navier solution. The values are taken from Reference[34].

For the clamped plate, the solution is obtained by combining the known solution for a simply supported plate under a uniform load with that of a plate bent by moments distributed along the pairs of opposite sides. The two solutions have been combined so as to satisfy all the requirements of the clamped edges. The values of strains (moments) and deflections are taken from Reference[34].

TABLE 1 - b

PLATE PARAMETERS

Plate No.	Thickness		
1	.0256"	30.04×10^6 psi	0.278 lb/in^3
2	.0598"	30.1×10^6 psi	0.277 lb/in^3
3	.0836"	30.06×10^6 psi	0.271 lb/in^3

TABLE 1 - a

COMPARISON OF STATIC & DYNAMIC DEFLECTIONS

Thickness of Plate in inches	Clamped - Clamped Plate			Simply Supported Plate		
	Non-dimensionalised deflection.		Dynamic deflection inches	Non-dimensionalised deflection		Dynamic deflection inches
	Static	Dynamic		Static	Dynamic	
0.0256"	.00245	.00475295	.0263988	.00772	.0155418	.0863222
0.0598"	.00245	.00473937	.0020651	.00772	.0158325	.00691212
0.0836"	.00245	.00453814	.0007237	.00772	.0157627	.00251394

TABLE - 2

Actual pressure on the plate for holes of shape 1

Pressure in the high pressure chamber psi	Shape	Ratio A_2/A_1	Pressure on the plate psi	t_1 m.sec.	t_2 m.sec
6	1	0	5.6	4.6	7.0
		1/64	5.2	3.6	5.8
		1/16	4.48	3.6	5.6
		1/4	3.4	3.6	5.6
8	1	0	7.0	4.6	7.0
		1/64	6.7	4.6	7.2
		1/16	6.2	4.6	7.4
		1/4	4.7	4.6	7.0
10	1	0	8.8	4.6	7.0
		1/64	8.5	4.6	8.0
		1/16	7.8	4.6	8.0
		1/4	6.2	4.6	7.0

TABLE - 3

Actual pressure on the plate for holes of shape 2

Pressure in H.P. chamber psi	Shape	Ratio A_2/A_1	Pressure on the plate psi	t_1 m.sec.	t_2 m.sec.
6	2	0	5.6	4.6	7.0
		1/64	5.3	3.6	5.6
		1/16	4.8	4.4	7.0
		1/4	3.4	4.6	7.0
8	2	0	7.0	4.6	7.0
		1/64	6.8	4.6	7.2
		1/16	6.36	4.6	7.0
		1/4	4.6	4.6	7.0
10	2	0	7.0	4.6	7.0
		1/64	6.8	4.6	7.2
		1/16	7.8	4.6	7.8
		1/4	6.0	4.6	8.0

TABLE - 4

Actual Pressure on the plate for holes of shape 3

Pressure in H.P. chamber psi	Shape	Ratio A_2/A_1	Pressure on the plate psi	t_1 m.sec.	t_2 m.sec.
6	3	0	5.6	4.6	7.0
		1/64	5.24	3.6	5.6
		1/16	4.6	3.6	5.6
		1/4	3.4	3.6	5.6
8	3	0	7.0	4.6	7.0
		1/64	6.8	4.6	7.0
		1/16	6.2	4.6	7.4
		1/4	4.6	4.6	7.0
10	3	0	8.3	4.6	7.0
		1/64	8.6	4.6	8.0
		1/16	7.9	4.6	7.7
		1/4	6.2	4.6	7.8

TABLE 5

Comparision of theoretical static and dynamic strains with experimental dynamic strains

Thickness = 0.0256 in. a = 4 in. b = 3 in.

(a)

Pressure on the plate	$-e_x$ (0,3)			$-e_y$ (2,0)		
	Dynamic		Static	Dynamic		Static
	Exp.	Theor.		Exp.	Theor.	
psi	μ in/in	μ in/in	μ in/in	μ in/in	μ in/in	μ in/in
5.6	932.0	3254.0	2074.0	896.0	1910.0	1511.0
7.0	1465.0	4070.0	2592.0	1320.0	2386.0	1890.0
8.8	1965.0	5110.0	3258.0	1548.0	3005.0	2376.0

(b)

Pressure on the plate	e_x (2, 3)			e_y (2, 3)		
	Dynamic		Static	Dynamic		Static
	Exp.	Theor.				
psi	μ in./in	μ in/in	μ in/in	μ in/in	μ in/in	μ in/in
5.6	-	2085.0	840.0	-	672.0	253.8
7.0	-	2612.0	1050.0	-	840.0	3174.0
8.8	-	3284.0	1320.0	-	1053.0	3988.0

TABLE 6

Comparision of theoretical static and dynamic strains with experimental dynamic strains

Thickness = 0.0598 in. a = 4 in. b = 6 in.

(a)

Pressure on the plate	$-e_x$ (0,3)			$-e_y$ (2,0)		
	Dynamic		Static	Dynamic		Static
	Exp.	Theor.		Exp.	Theor.	
psi	μ in/in	μ in/in	μ in/in	μ in/in	μ in/in	μ in/in
5.6	447.0	592.0	382.8	278.4	386.2	284.4
7.0	578.1	739.3	479.0	386.0	483.0	356.0
8.8	629.0	930.0	601.1	499.5	607.0	404.7

(b)

Pressure on the plate	e_x (2,3)			e_y (2,3)		
	Dynamic		Static	Dynamic		Static
	Exp.	Theor.		Exp.	Theor.	
psi	μ in/in	μ in/in	μ in/in	μ in/in	μ in/in	μ in/in
5.6	323.0	382.8	153.8	204.4	175.8	46.4
7.0	402.0	478.0	192.3	228.6	219.4	58.1
8.8	484.0	601.5	241.9	290.0	276.0	72.91

TABLE 7

Comparision of theoretical static and dynamic strains with experimental dynamic strains

Thickness = 0.0836 in. a = 4 in. b = 6 in.

(a)

Pressure on the plate	$-e_x$ (0,3)			$-e_y$ (2,0)		
	Dynamic		Static	Dynamic		Static
	Exp.	Theor.		Exp.	Theor.	
psi	μ in/in	μ in/in	μ in/in	μ in/in	μ in/in	μ in/in
5.6	219.2	298.2	194.2	182.1	207.6	146.1
7.0	290.4	382.6	242.6	245.4	259.5	182.9
8.8	353.4	468.5	298.0	326.8	326.4	229.8

(b)

Pressure on the plate	e_x (2,3)			e_y (2,3)		
	Dynamic		Static	Dynamic		Static
	Exp.	Theor.		Exp.	Theor.	
psi	μ in/in	μ in/in	μ in/in	μ in/in	μ in/in	μ in/in
5.6	168.1	193.5	83.15	96.7	85.9	23.74
7.0	222.8	242.0	103.9	145.1	107.6	29.68
8.8	252.6	304.2	130.8	161.5	135.1	37.31

TABLE - 8

EXPERIMENTAL RESULTS FOR STRAINS AT THE ENDS FOR CLAMPED PLATE

Thickness = 0.0256" a = 4 in. b = 6 in.

E_x Strain in the x - direction at point (0, 3)

E_y Strain in the y - direction at point (2, 0)

Strains are in micro inch/inch.

pe	Pressure psi	A_2/A_1 1/64		1/16		1/4		0	
		$-e_x$	$-e_y$	$-e_x$	$-e_y$	$-e_x$	$-e_y$	$-e_x$	$-e_y$
	3.4	879.2	586.0	920.0	482.0	707.0	646.0	566.0	545.0
	4.6	1070.0	665.0	1062.0	656.0	1059.0	895.0	963.0	867.0
	6.2	1442.0	735.0	1470.0	909.0	1380.0	1228.0	1385.0	1091.0
	3.4	735.0	557.0	711.0	569.0	493.0	775.0	566.0	545.0
2	4.6	841.3	617.0	943.0	715.0	698.0	1198.0	963.0	867.0
	6.2	941.0	736.0	1278.0	980.0	896.0	1320.0	1385.0	1091.0
	3.4	820.4	507.0	874.0	491.0	468.0	726.0	566.0	545.0
3	4.6	982.3	647.5	1265.0	734.0	585.0	917.0	963.0	867.0
	6.2	1408.3	820.0	1622.0	884.0	700.0	1054.0	1385.0	1091.0

TABLE - 9

EXPERIMENTAL RESULTS FOR STRAINS AT THE ENDS FOR CLAMPED PLATE

Thickness = 0.0598" a = 4 in. b = 6 in.

E_x Strain in the x - direction at point (0, 3)

E_y Strain in the y - direction at point (2, 0)

Strains are in micro inch/inch.

Shape	Pressure psi	A_2/A_1	1/64	1/16		1/4		0	
		$-e_x$	$-e_y$	$-e_x$	$-e_y$	$-e_x$	$-e_y$	$-e_x$	$-e_y$
	3.4	288.0	152.5	282.6	140.4	257.2	221.0	270.8	169.0
1	4.6	390.8	246.0	386.8	214.8	391.8	307.2	380.0	253.9
	6.2	526.5	315.4	501.0	315.6	520.0	419.5	443.0	351.6
	3.4	237.9	170.0	298.2	214.0	179.6	310.6	270.8	169.0
2	4.6	297.9	258.2	388.4	273.4	258.4	442.0	380.0	253.9
	6.2	406.0	348.4	517.0	369.2	333.4	555.0	443.0	351.6
	3.4	317.8	177.6	343.0	173.9	178.8	281.0	270.8	169.0
3	4.6	439.0	252.4	487.0	230.4	244.4	394.4	380.0	253.9
	6.2	576.0	332.0	596.0	306.4	338.4	511.0	443.0	351.6

TABLE - 10

EXPERIMENTAL RESULTS FOR STRAINS AT THE ENDS FOR CLAMPED PLATE

Thickness = 0.0835" a = 4 in b = 6 in

E_x Strain in the x - direction at point (0, 3)

E_y Strain in the y - direction at point (2, 0)

Strains are in micro inch/inch.

Shape	Pressure psi	A_2/A_1	1/64		1/16		1/4		0	
		$-e_x$	$-e_y$	$-e_x$	$-e_y$	$-e_x$	$-e_y$	$-e_x$	$-e_y$
	3.4	137.0	103.2	127.2	6285	109.8	115.2	133.0	110.6
1	4.6	188.3	337.0	164.0	90.0	179.8	159.3	190.4	161.1
	6.2	260.2	191.0	246.0	130.8	232.0	204.6	248.8	230.3
	3.4	124.3	109.2	134.3	121.5	46.8	271.8	133.0	110.6
2	4.6	159.2	140.3	202.4	147.5	76.8	393.4	190.4	161.1
	6.2	221.8	181.1	281.2	195.5	113.0	533.8	248.8	230.3
	3.4	147.6	112.0	158.2	121.5	121.8	121.9	133.0	110.6
3	4.6	196.1	139.6	216.8	135.5	146.0	168.7	190.4	161.1
	6.2	266.6	188.0	301.0	181.5	191.0	215.6	248.8	230.3

TABLE - 11

PARAMETERS FOR A CLAMPED - CLAMPED MODE SHAPE

m or n	Generalised Mass M_m or M_n	Frequency Parameter $_m$ or $_n$	Resonance frequency parameter $_m$ $_n$	Maximum displacement $\overline{W}_m$ or $\overline{W}_n$	Modal co-efficient A_m or A_n
1	0.396	4.73004	12.302	1.6163	$1 + 1.78 \times 10^{-2}$
2	0.439	7.85320	46.050	1.5081	$1 - 7.76 \times 10^{-4}$
3	0.436	10.99560	98.905	1.5126	$1 + 3.40 \times 10^{-5}$
4	0.420	14.13720	171.590	1.5123	$1 - 2.45 \times 10^{-6}$
5	0.437	17.27880	264.138	1.5125	$1 + 6.27 \times 10^{-8}$
6	0.437	20.42035	376.109	1.5125	$1 - 2.71 \times 10^{-9}$
7	0.437	23.56195	506.863	1.5125	$1 + 1.18 \times 10^{-10}$
8	0.437	26.70354	659.405	1.5125	$1 - 5.09 \times 10^{-12}$
9	0.437	29.84513	830.743	1.5125	$1 - 9.34 \times 10^{-13}$

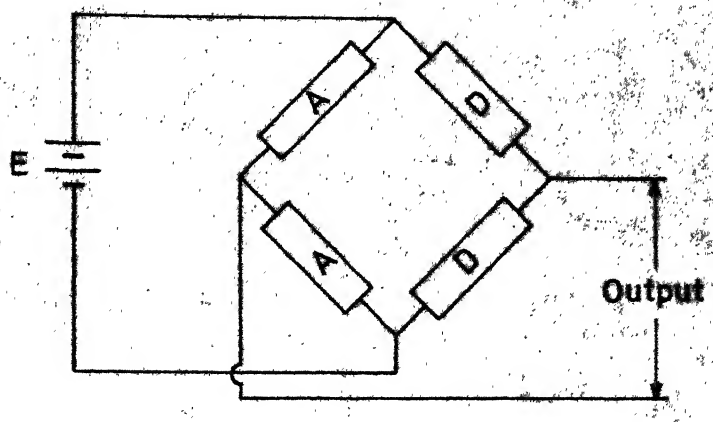

Fig. 1(a)

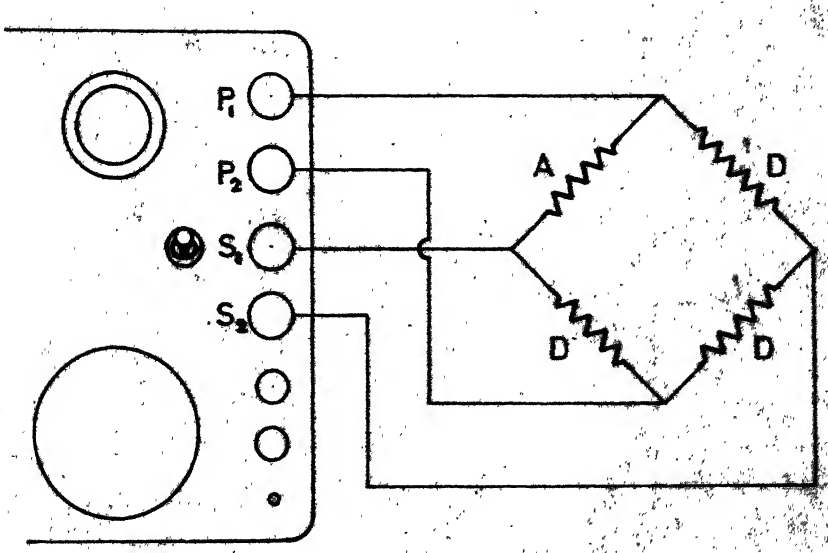

Fig. 1(b)

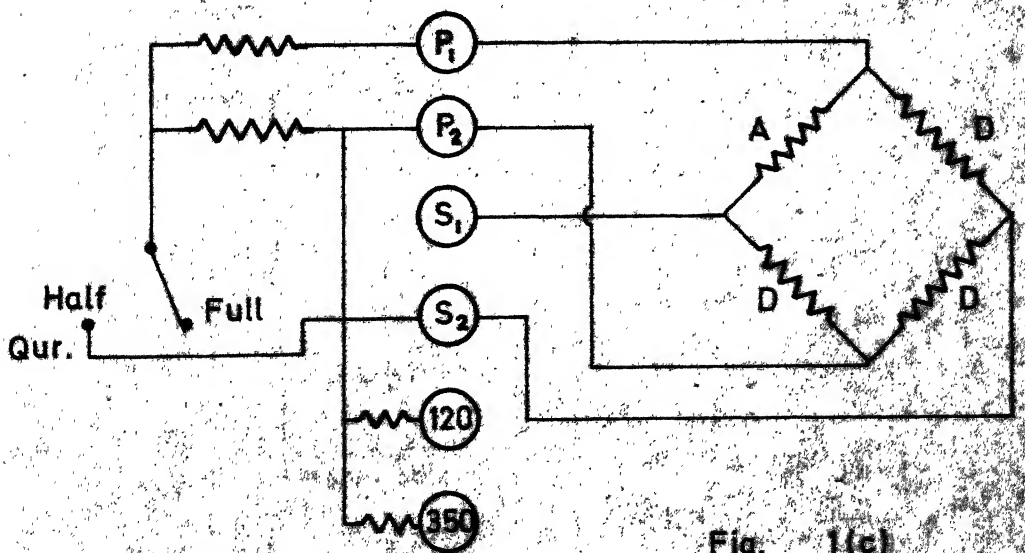

Fig. 1(c)

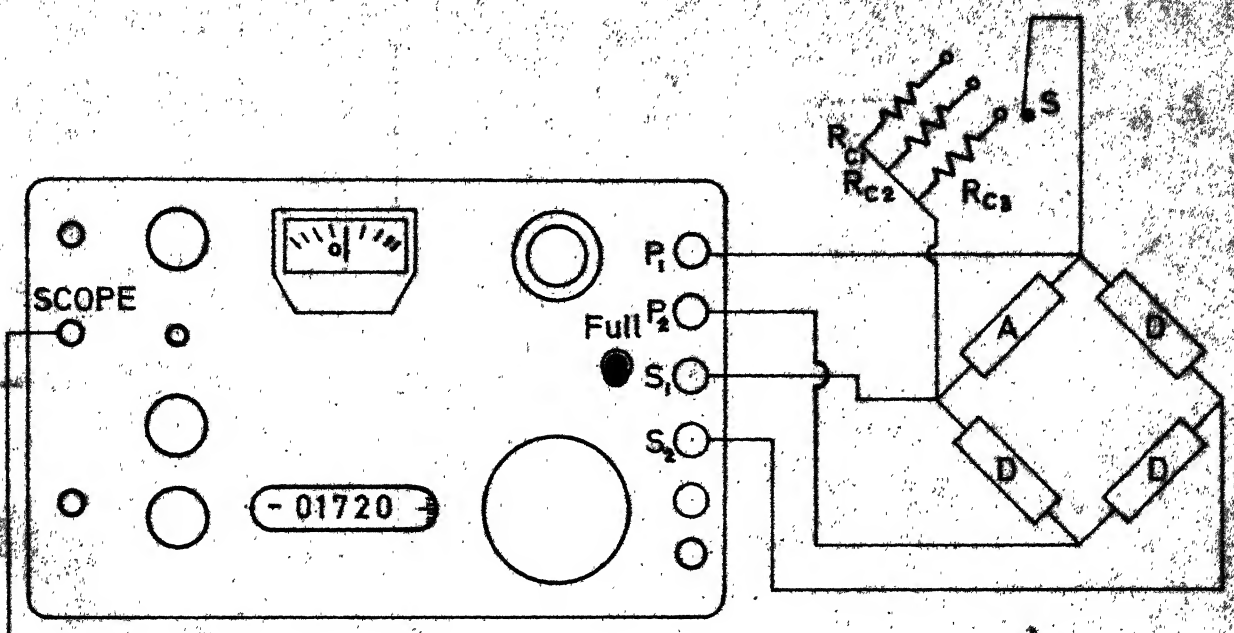

BUDD STRAIN INDICATOR

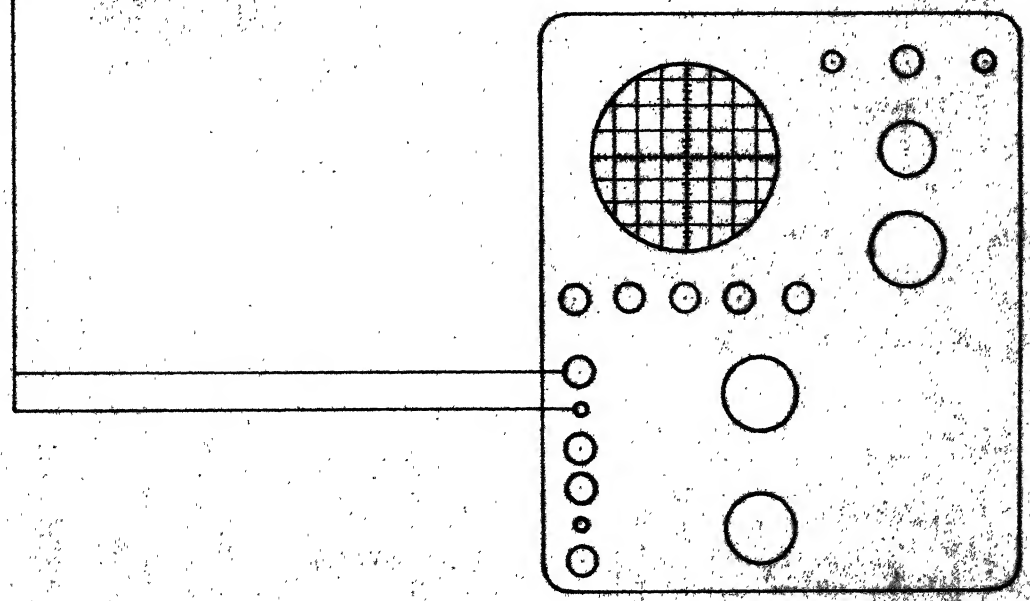

OSCILLOSCOPE

FIG. 3. STRAIN GAUGE CALIBRATION

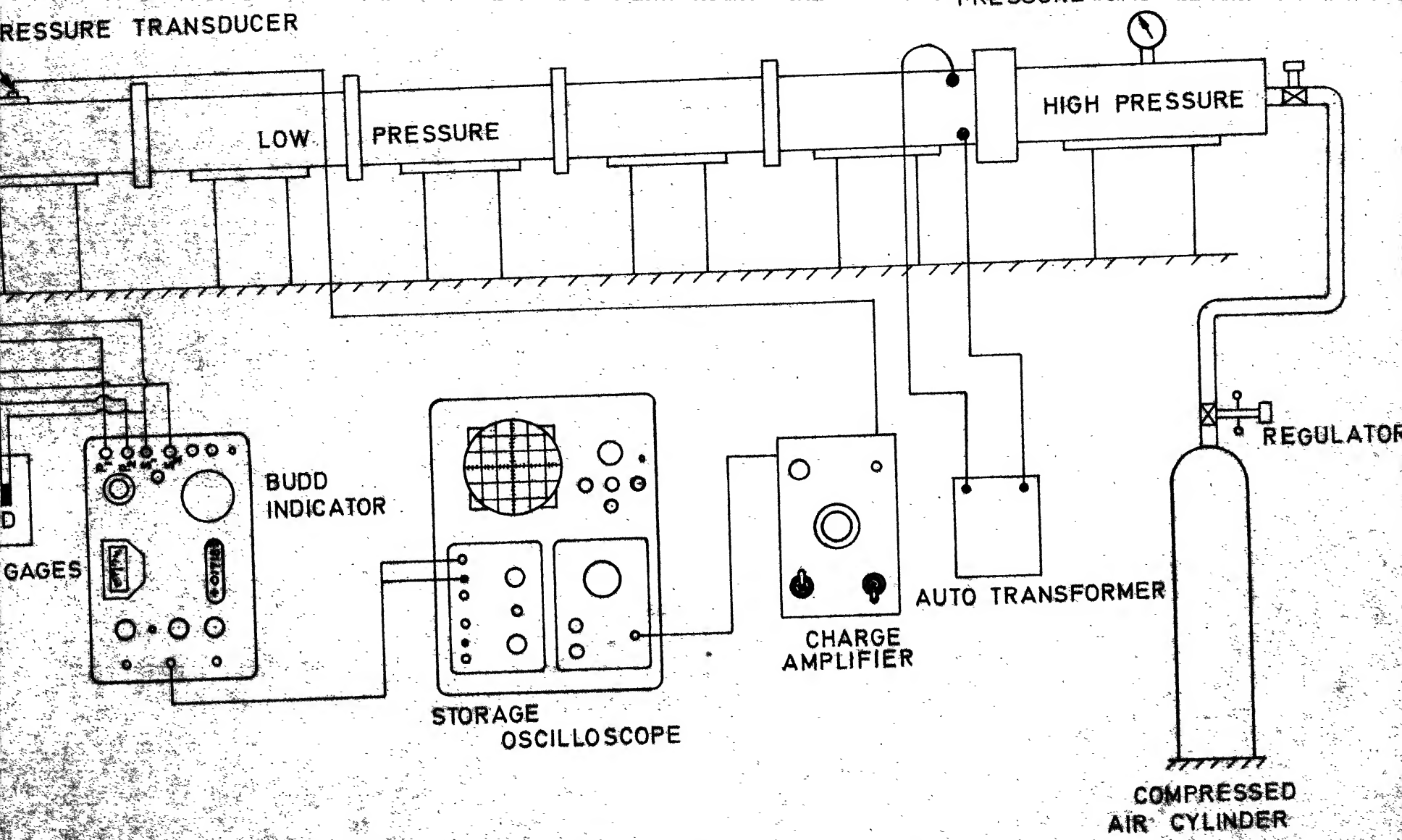

FIG. 4. STRAIN MEASUREMENT

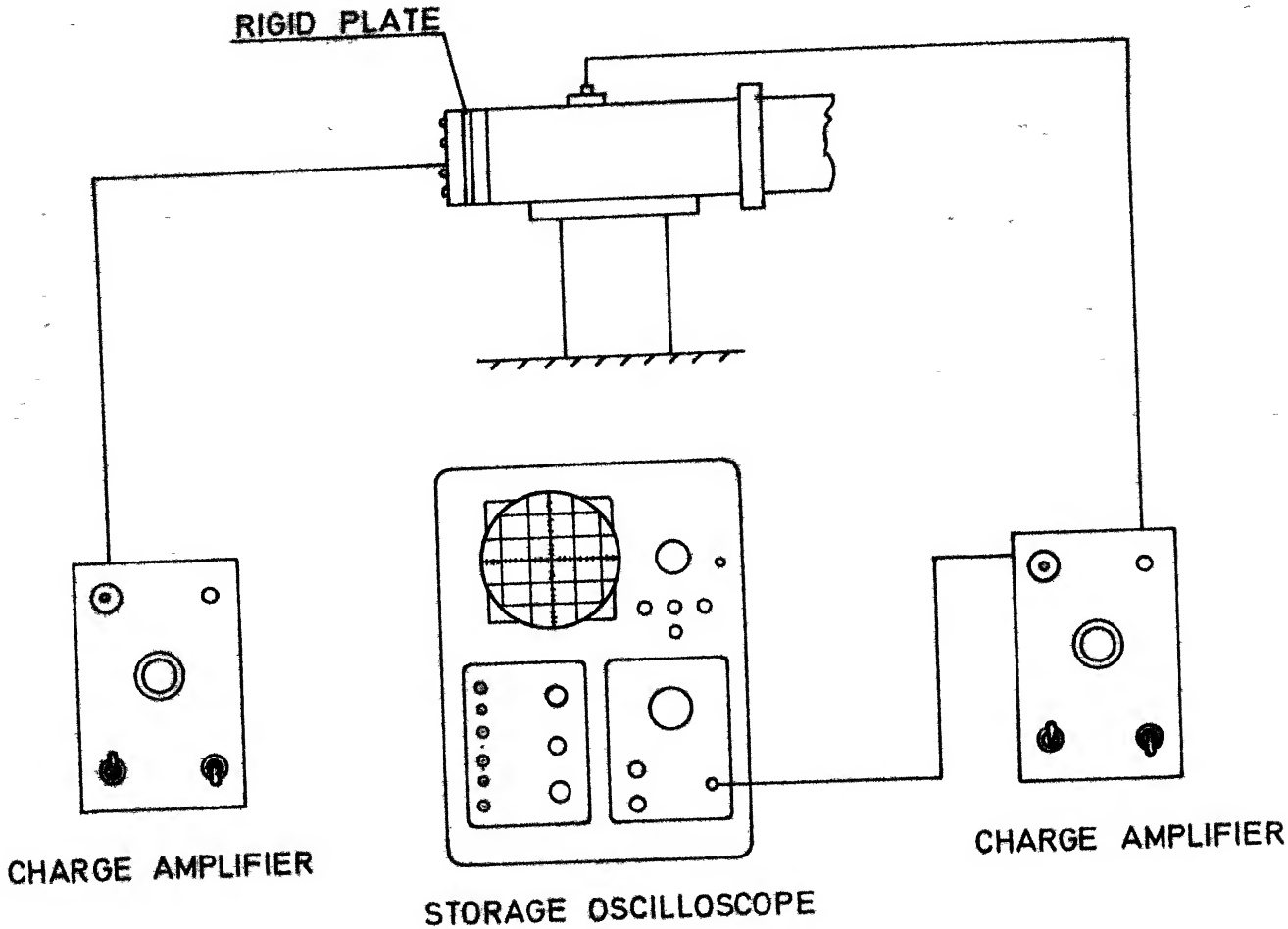

FIG. 5. PRESSURE MEASUREMENT

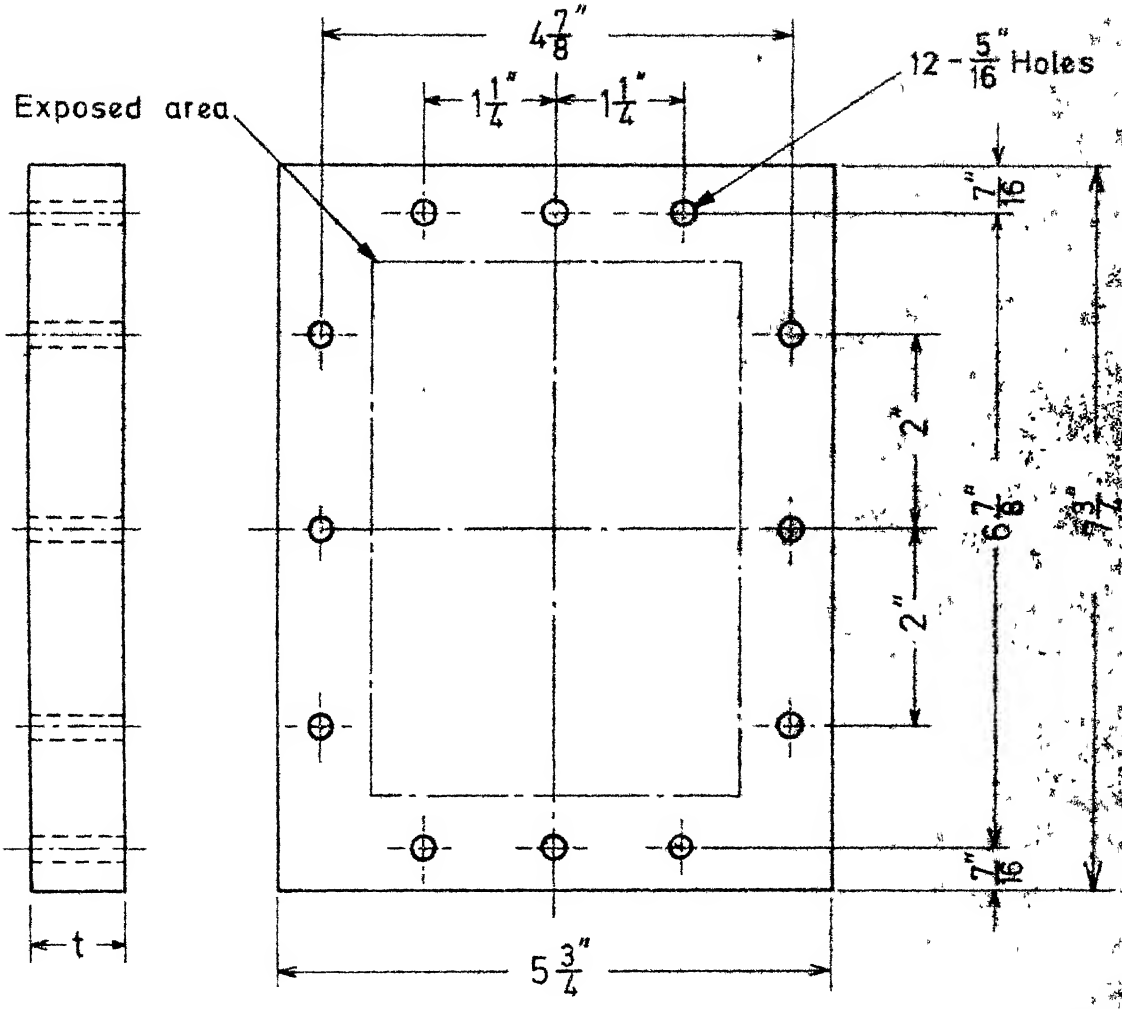

FIG. 6(a) TEST PLATE

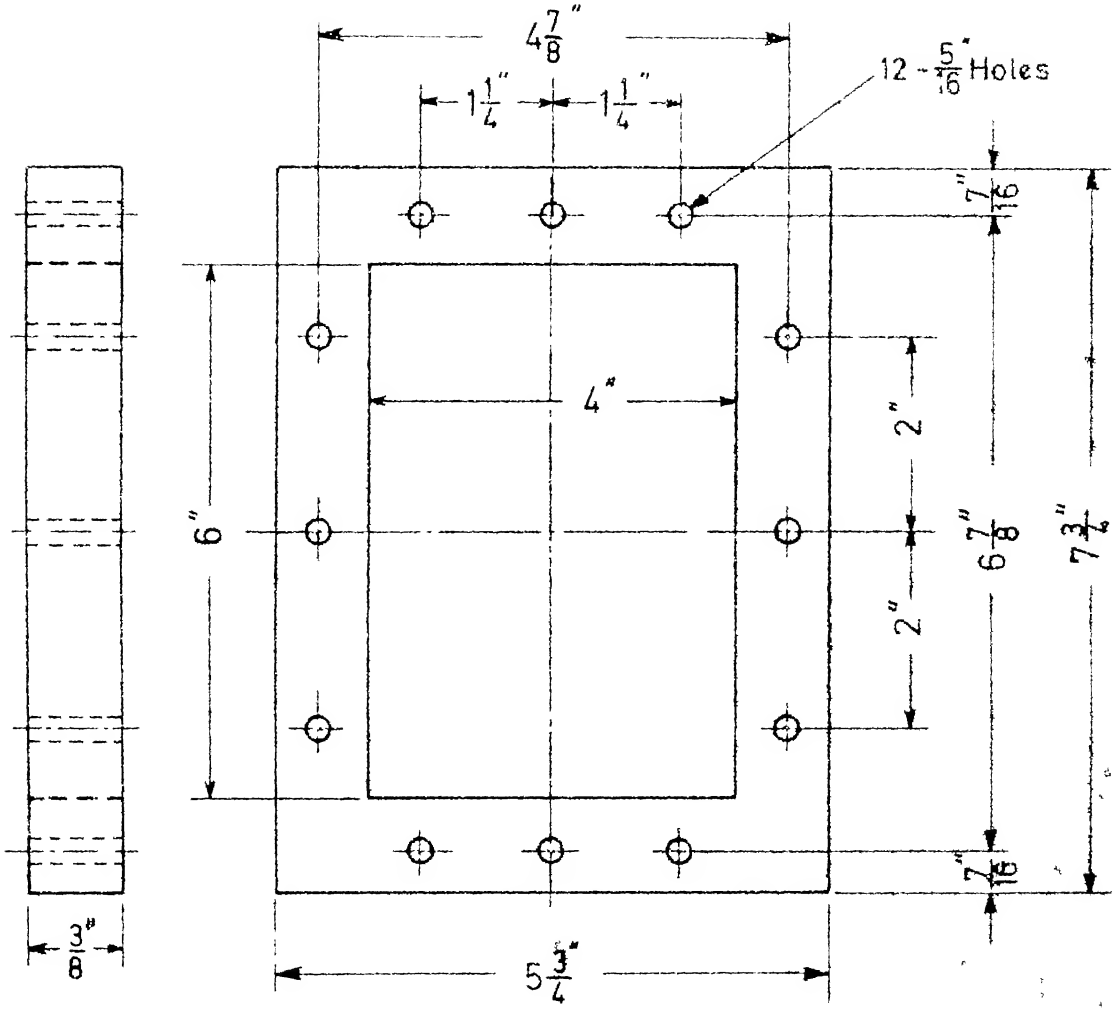

FIG 6(b) SUPPORTING FRAME

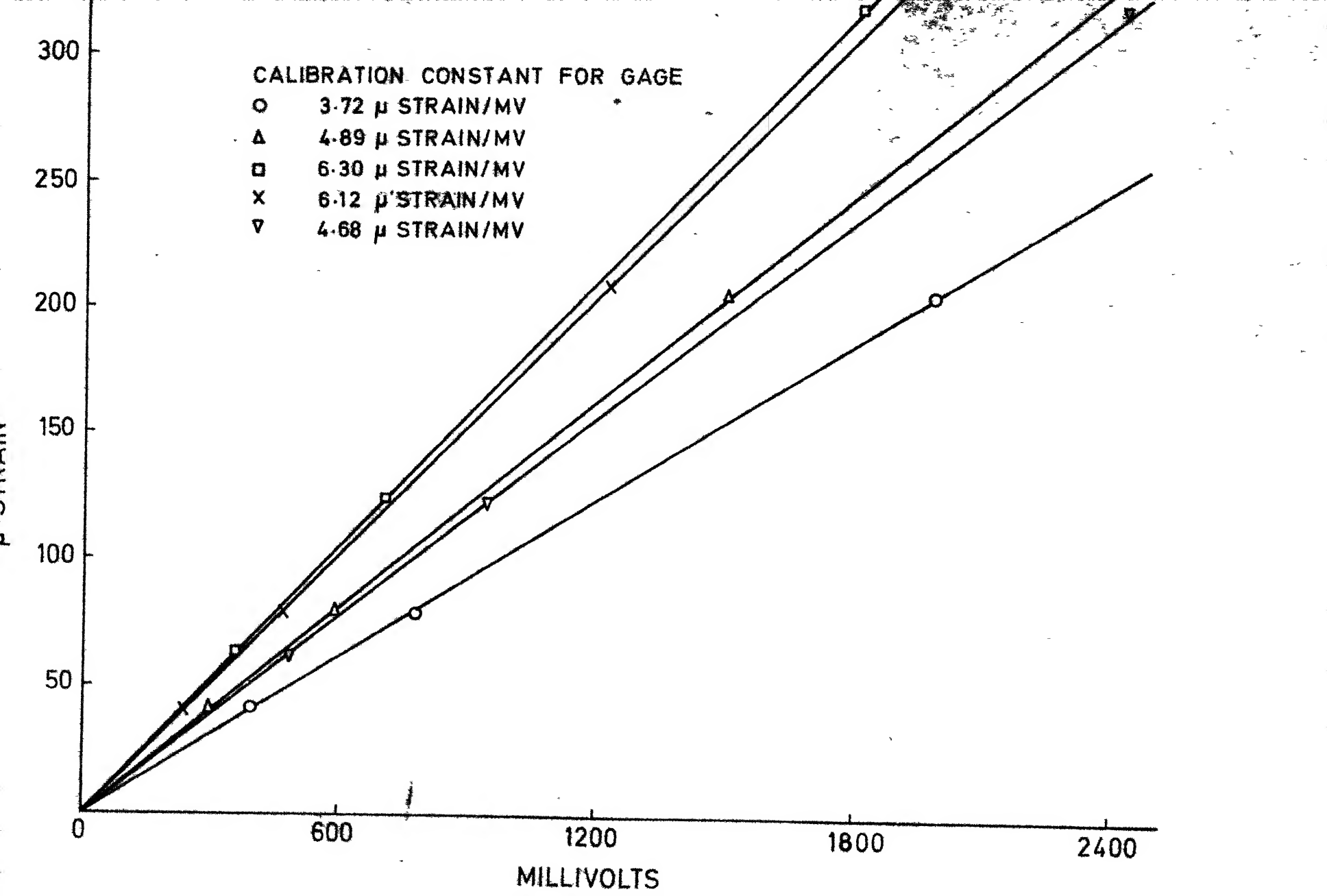
CALIBRATION CONSTANT FOR GAGE
○ 3·72 μ STRAIN/MV
△ 4·89 μ STRAIN/MV
□ 6·30 μ STRAIN/MV
× 6·12 μ STRAIN/MV
▽ 4·68 μ STRAIN/MV
300
250
200
150
100
50
0
600
1200
1800
2400
MILLIVOLTS

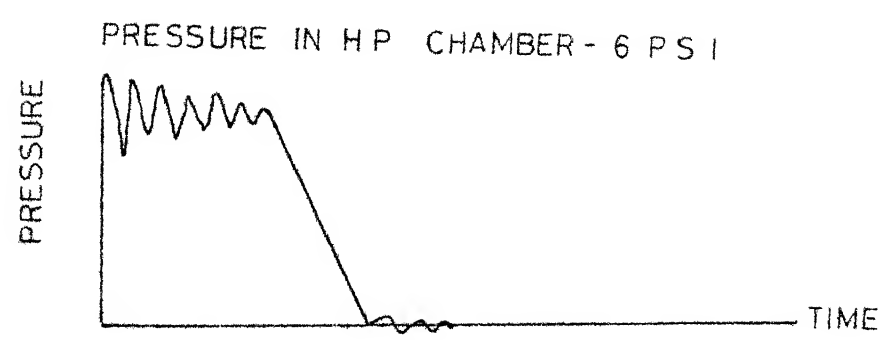

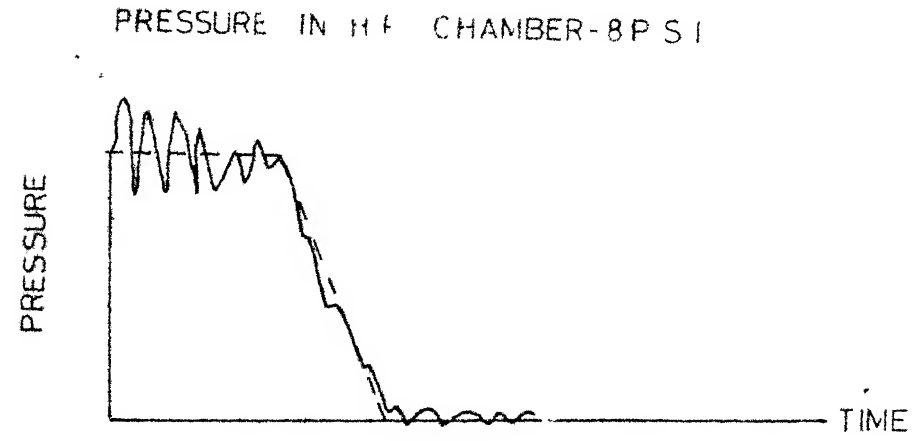

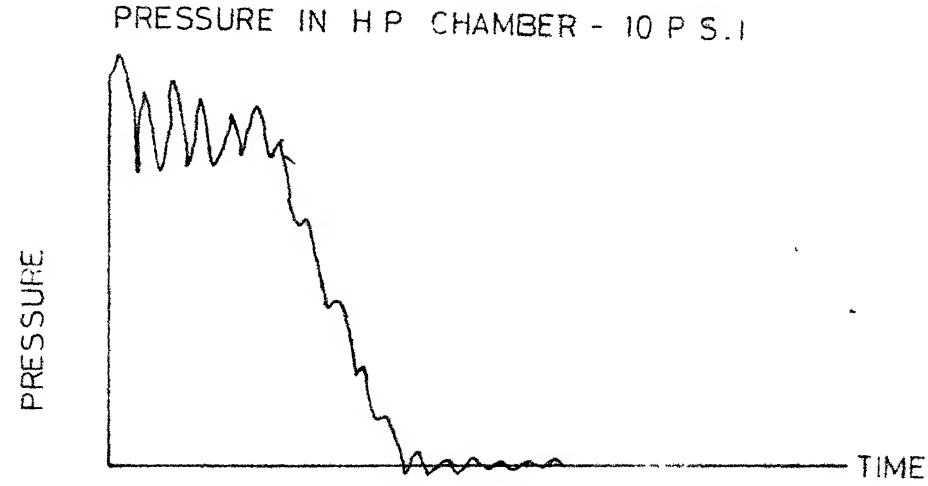

SENSITIVITY - 0 2 VOLTS/CM (100 MV/ P S I)
SWEEP 2 MSEC / CM

FIG 8 PRESSURE VS. TIME

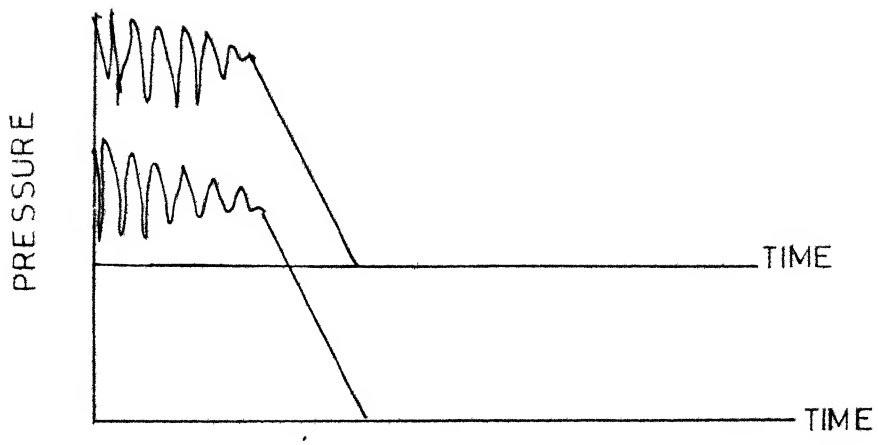

FIG SHOWS THAT THE NATURE OF SHOCK WAVE IS PLANE
FIG 9a

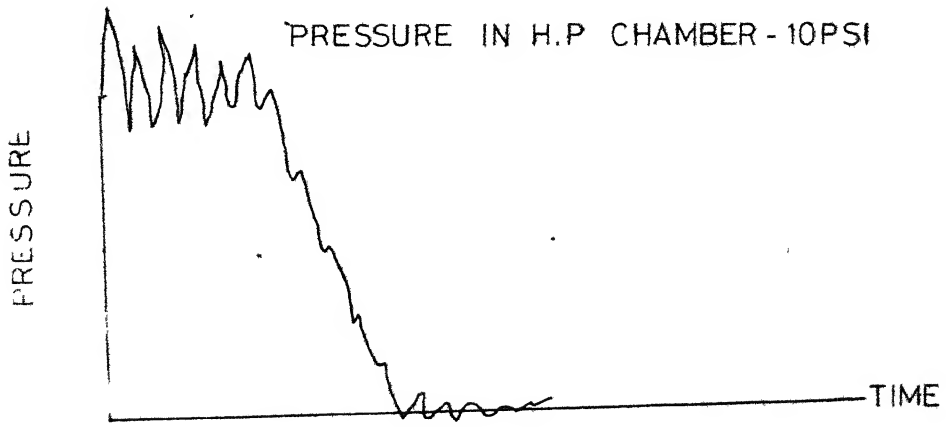

PRESSURE DISTRIBUTION WITHOUT AN OPENING.

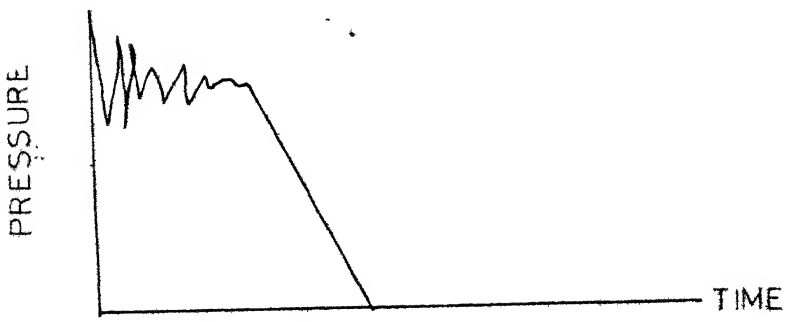

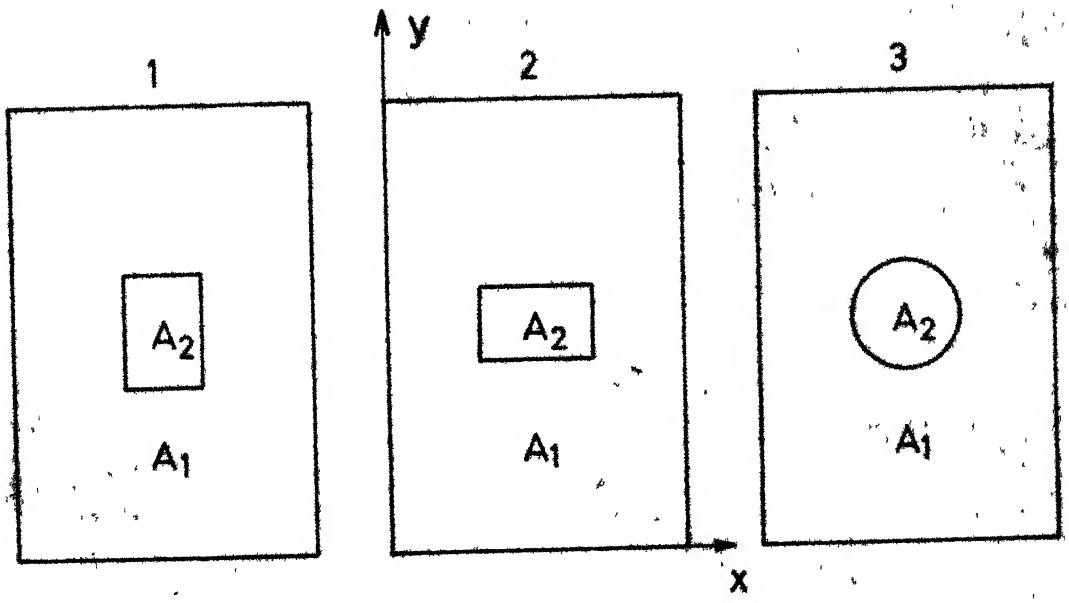

TYPES OF HOLES

FIG. 10.

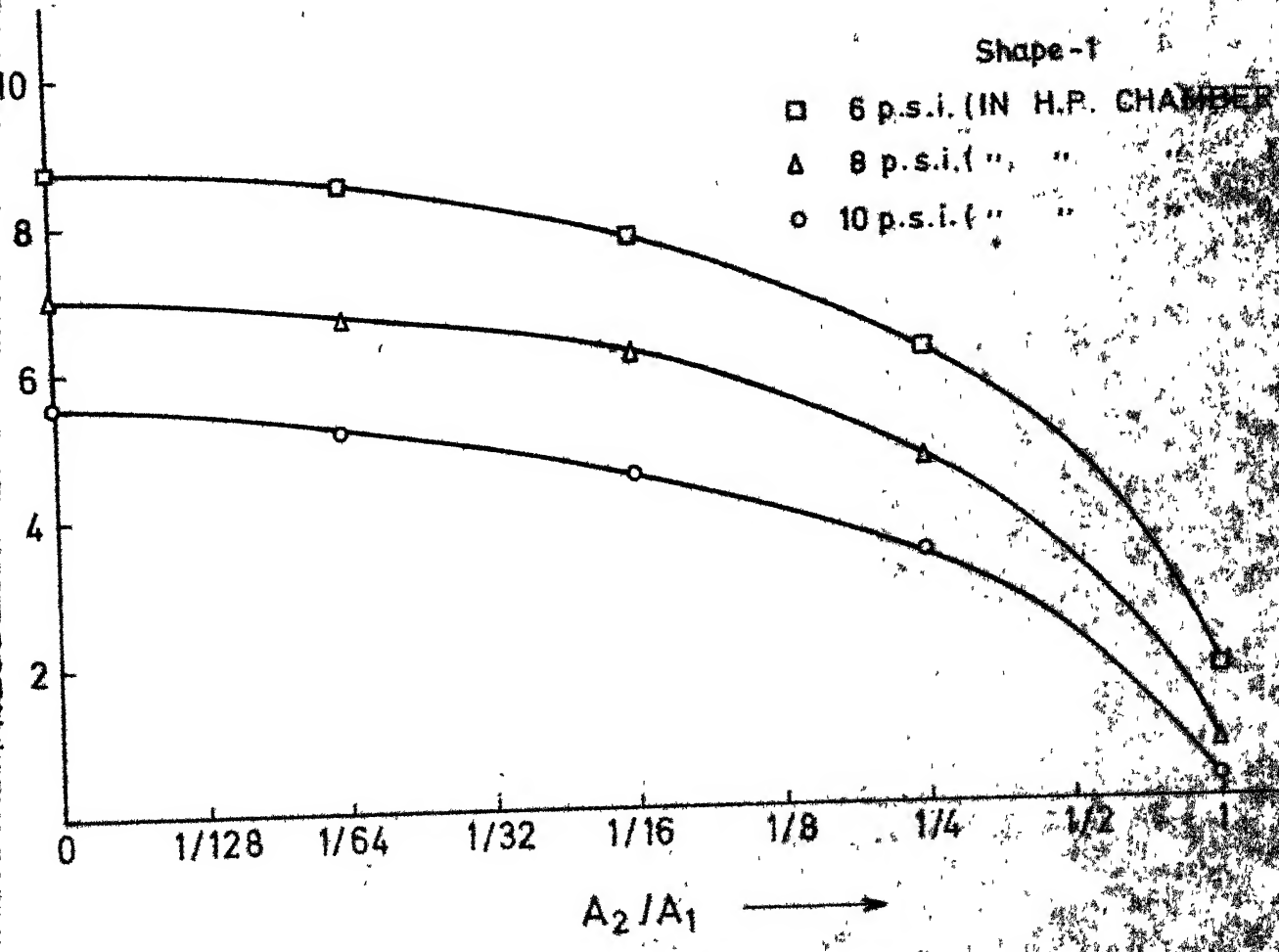

FIG. 11(a).

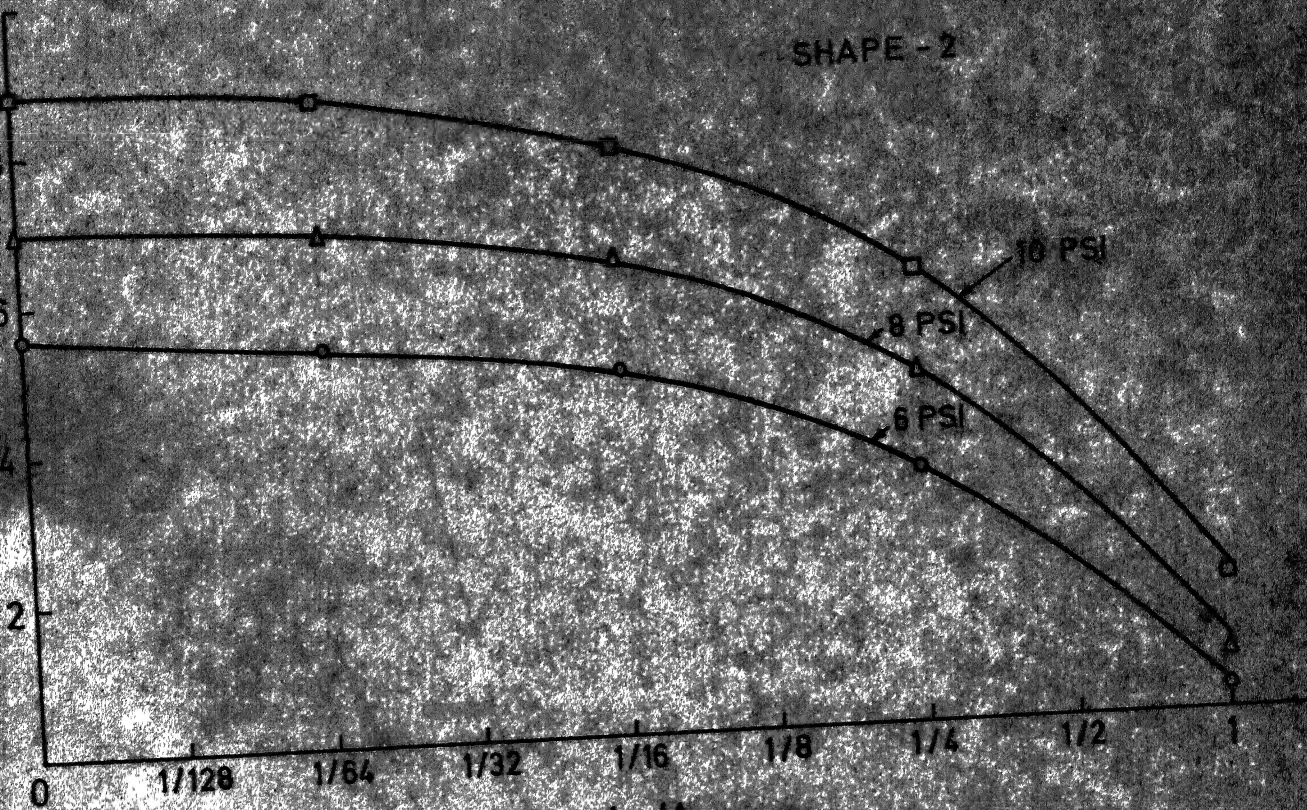
SHAPE - 2
10 PSI
8 PSI
6 PSI
2
4
0
1/128
1/64
1/32
1/16
1/8
1/4
1/2
1
A_2/A_1

FIG. 11 (b).

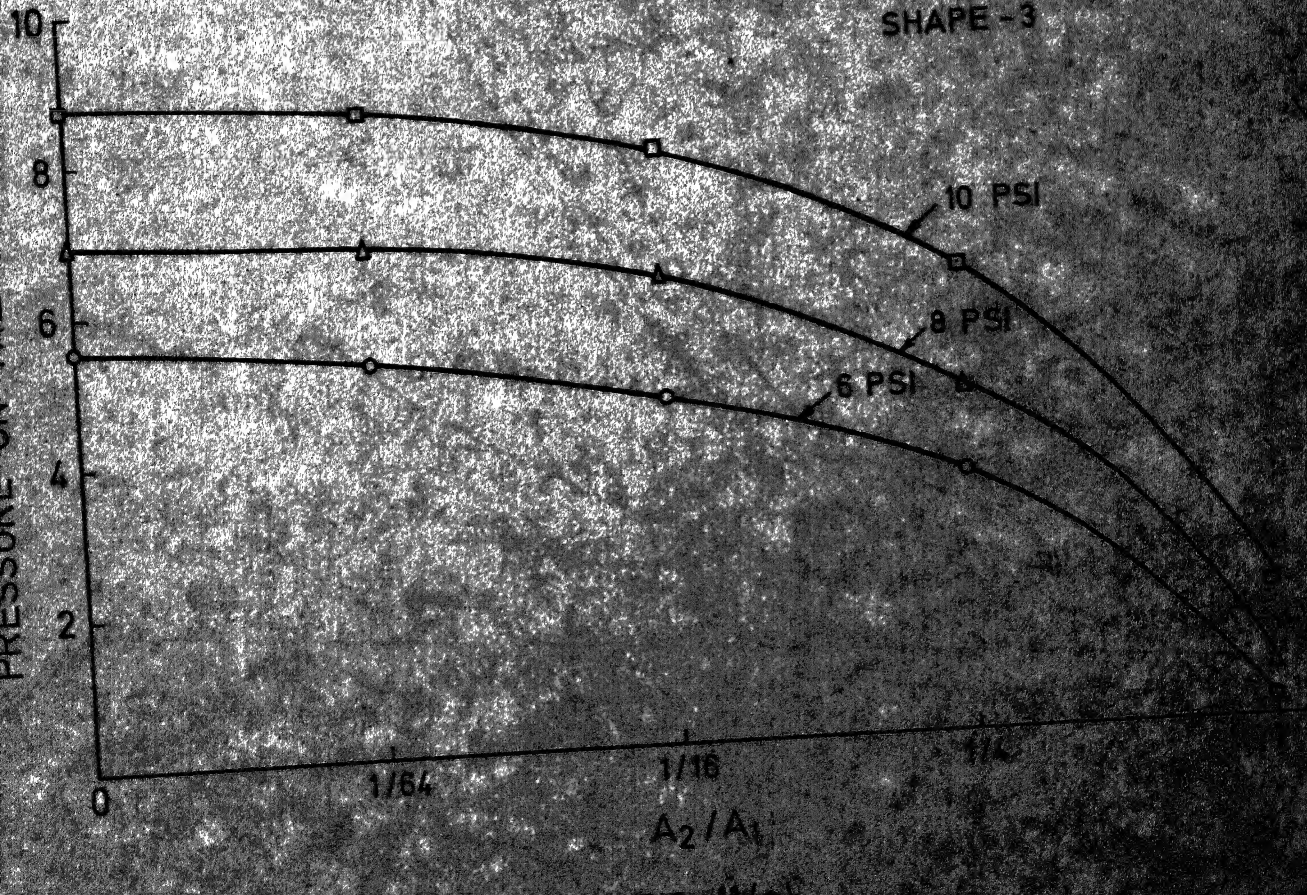
SHAPE - 3
10
8
6
4
2
0
10 PSI
8 PSI
6 PSI
1/64
1/16
A_2/A_1

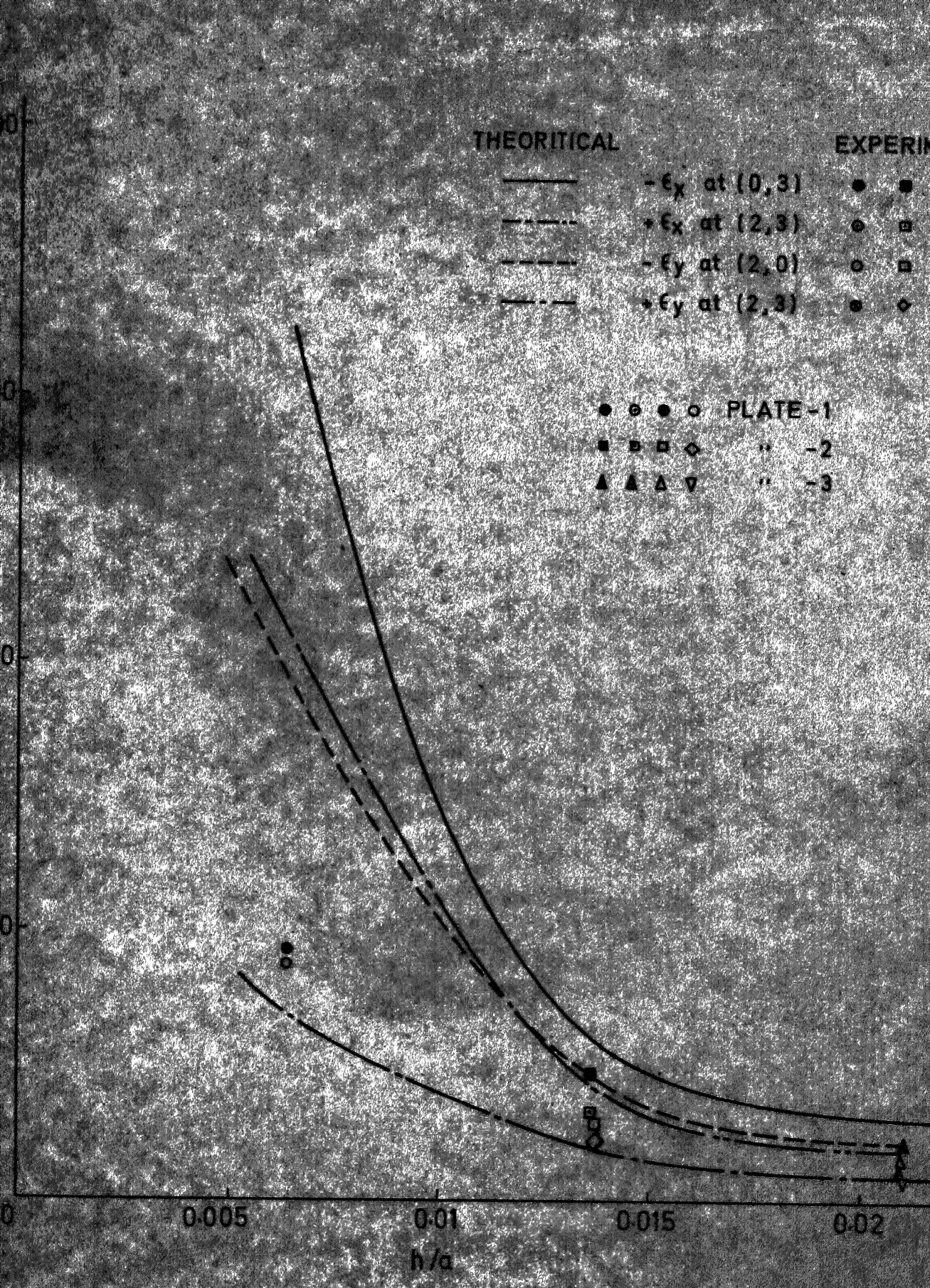

FIG. 12. COMPARISON OF THEORITICAL AND EXPERIMENTAL STRA

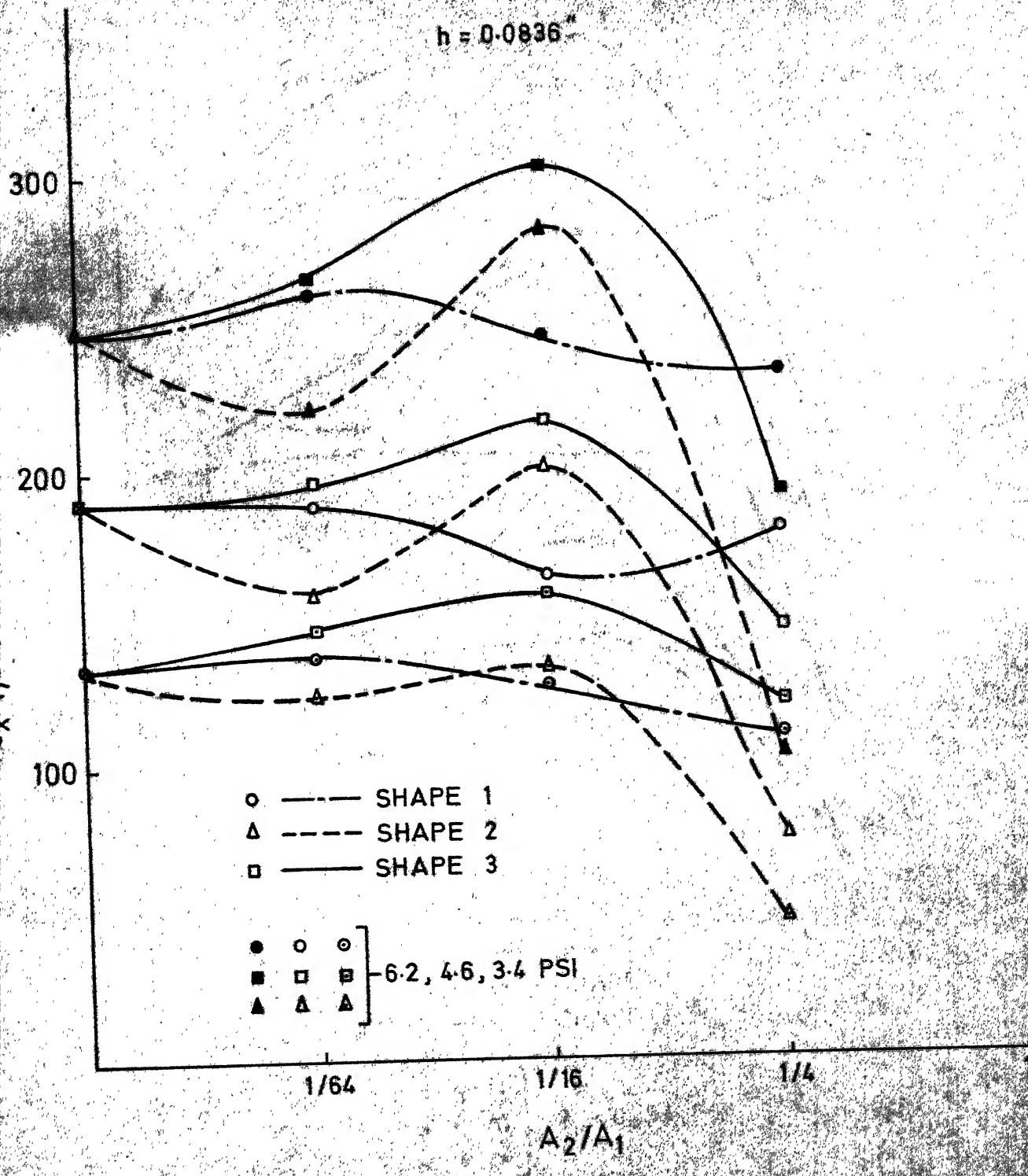

FIG. 13. ϵ_x Vs. AREA RATIO FOR PLATE 3.

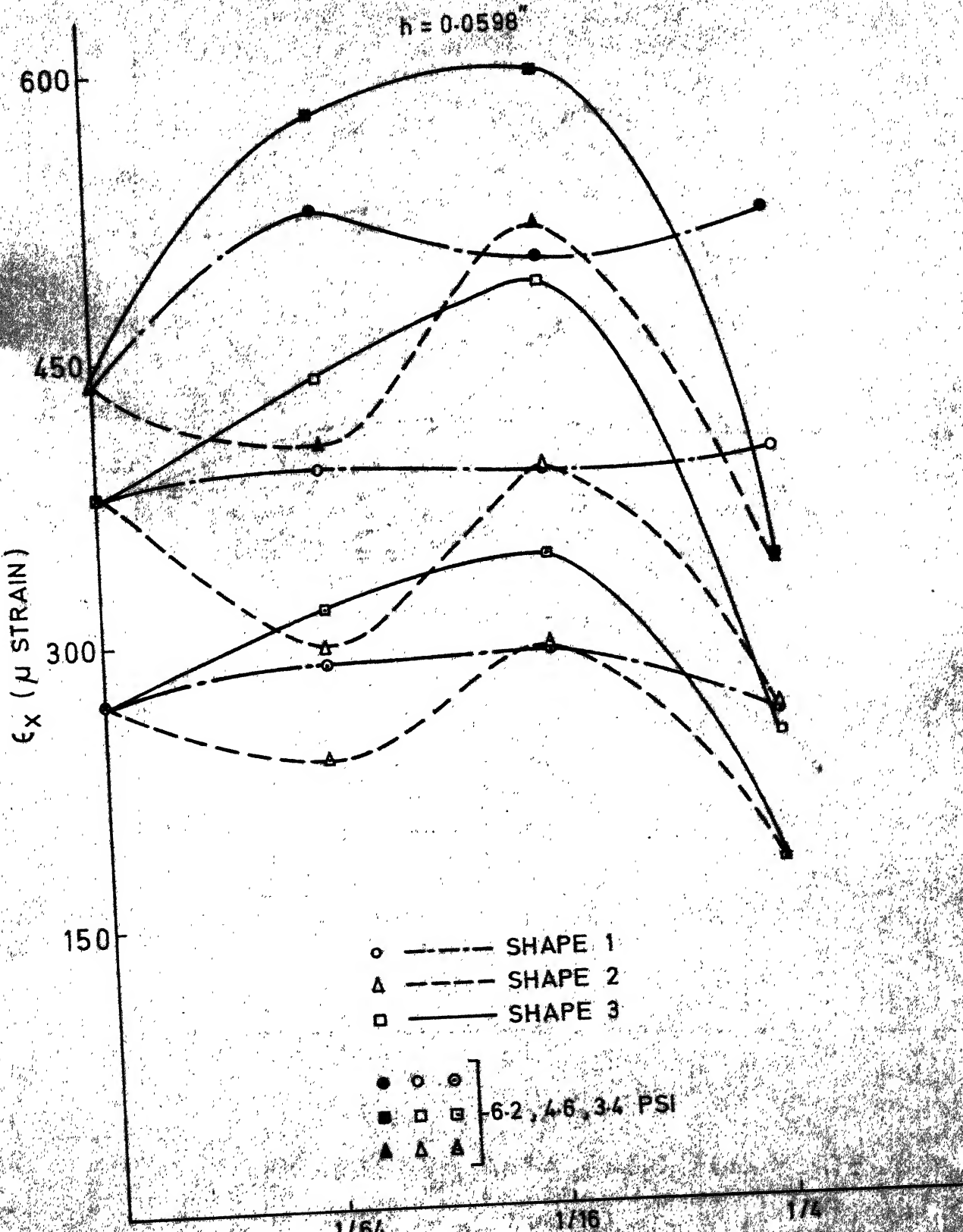

Fig 14 ϵ_x Vs. AREA RATIO FOR PLATE 2.

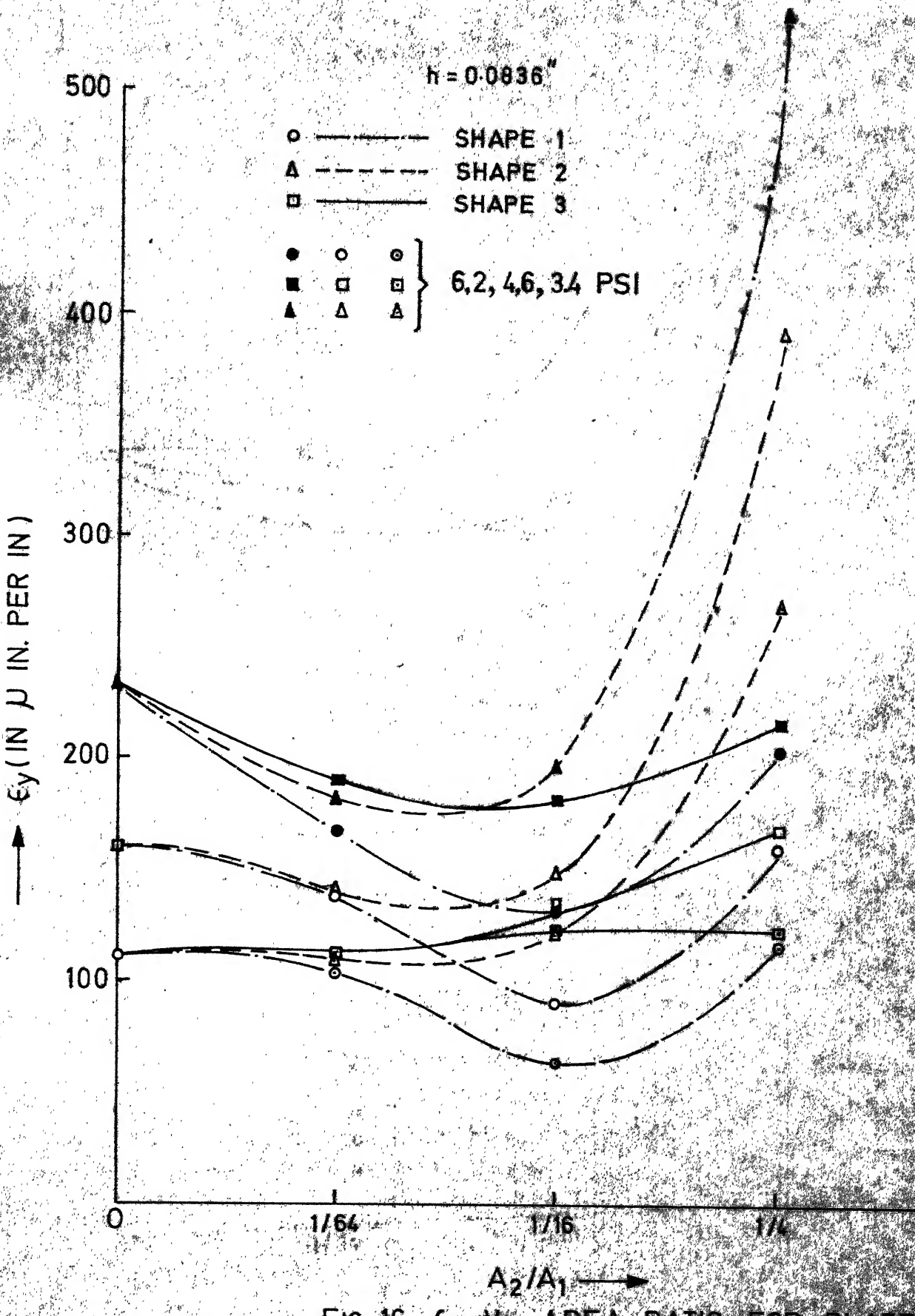

FIG. 16 ϵ_y Vs. AREA RATIO FOR PLATE

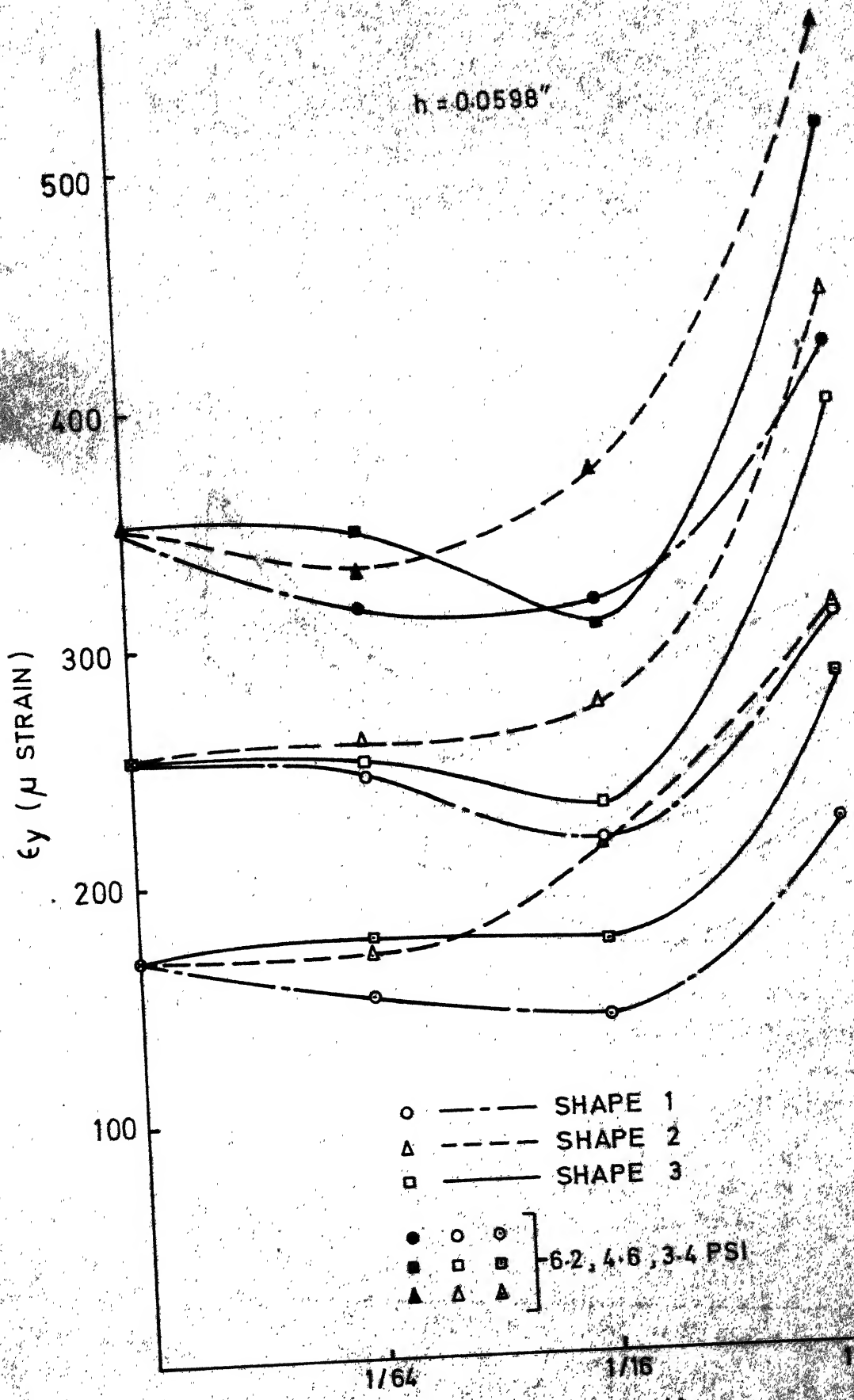

AREA RATIO FOR PLATE 2.

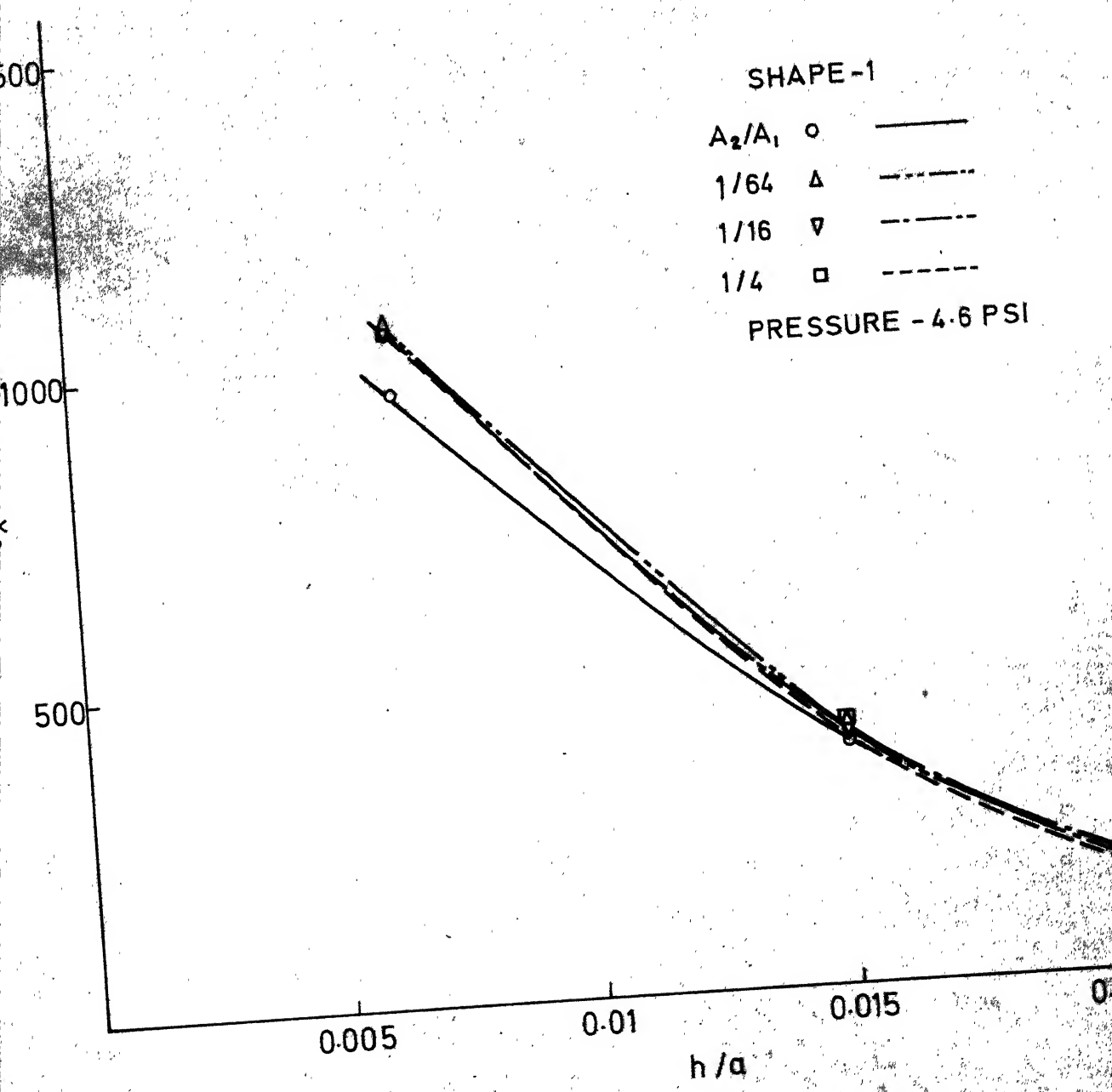

FIG. 19(a) ϵ_x Vs. h/a

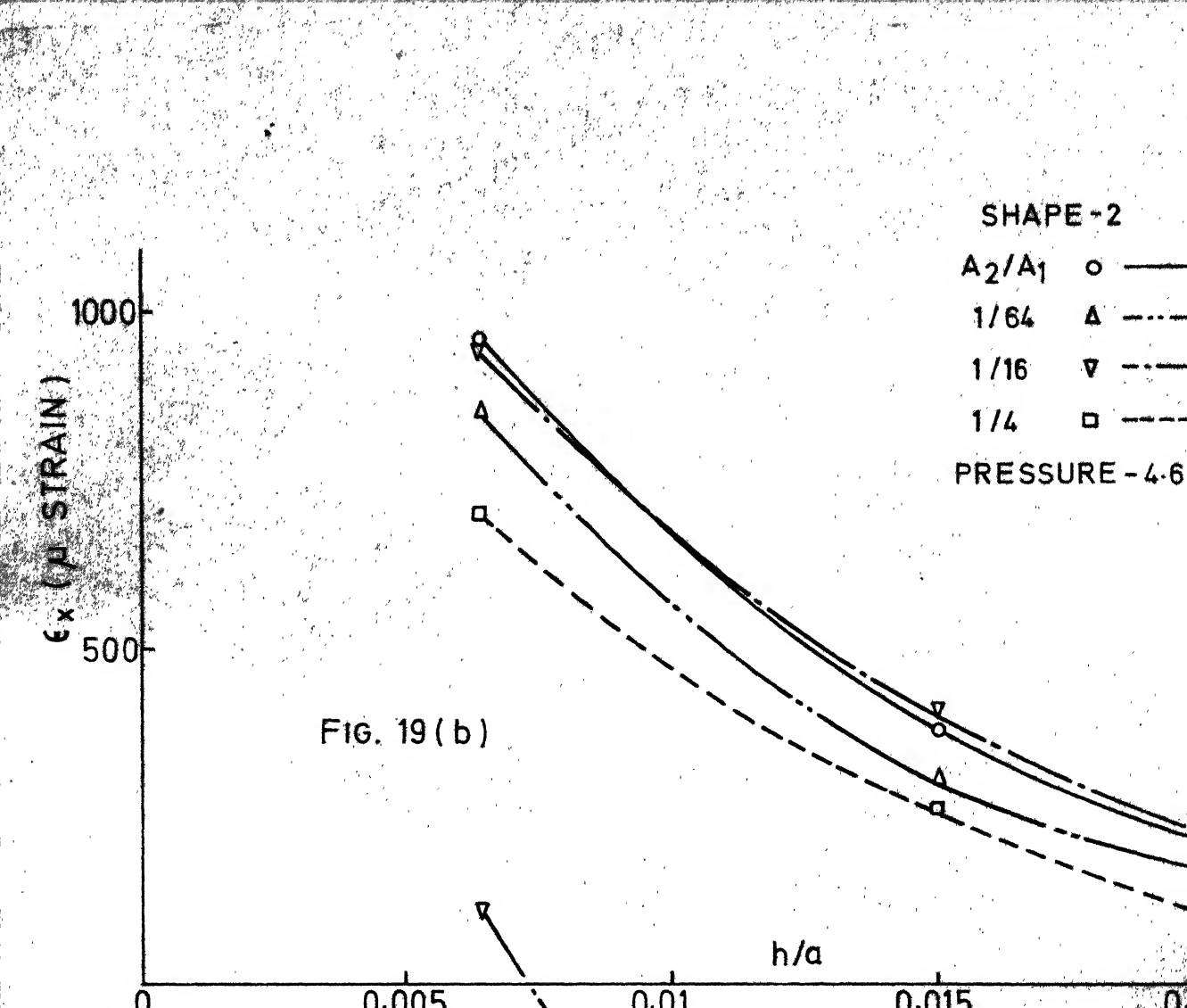

FIG. 19 (b)

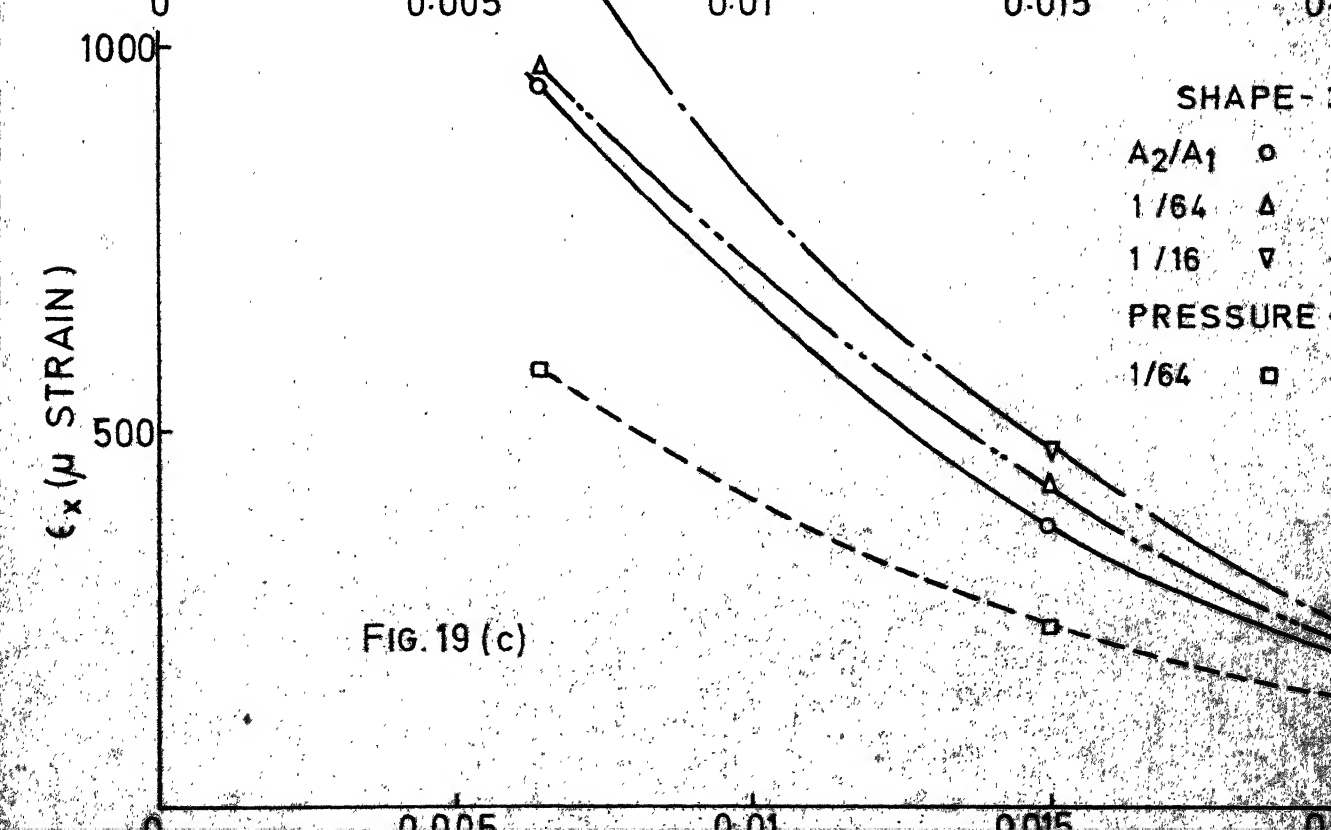

FIG. 19 (c)

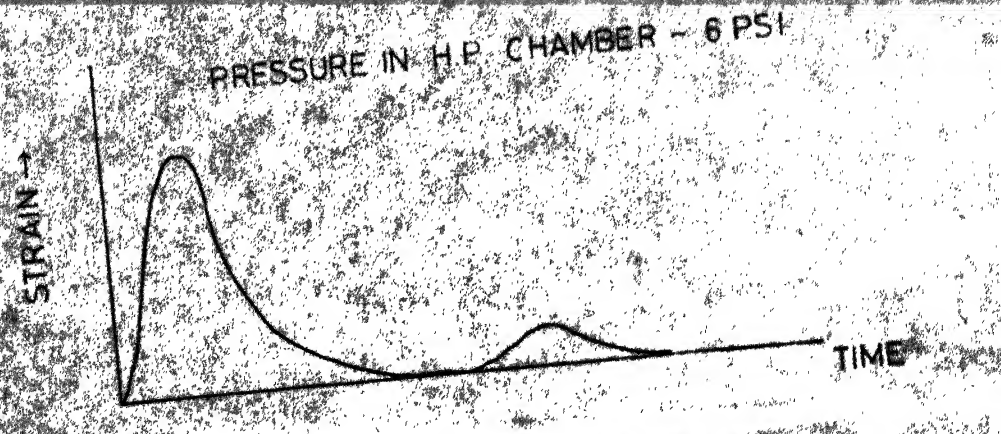

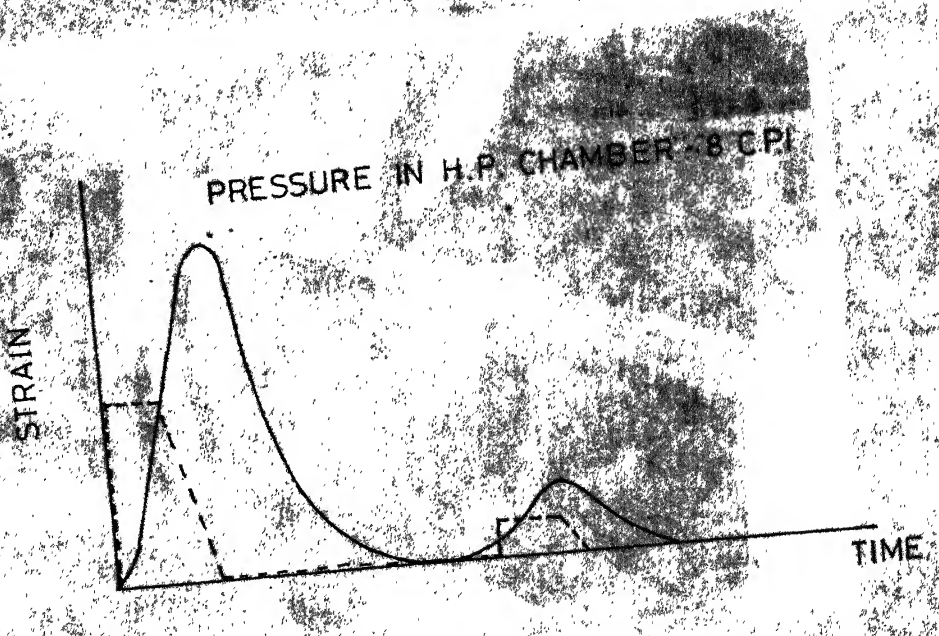

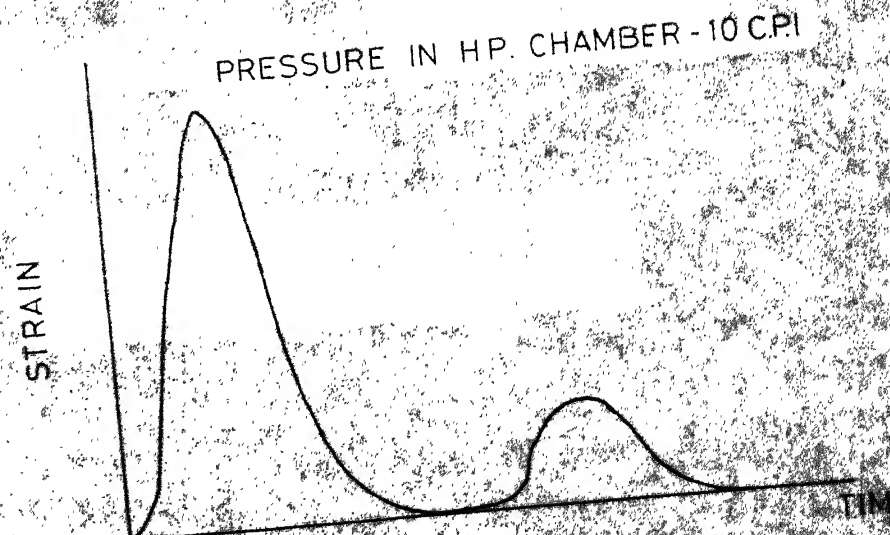

SENSITIVITY 20 mv/cm
SWEEP 5 msec/cm

FIG. 20. STRAIN VS TIME

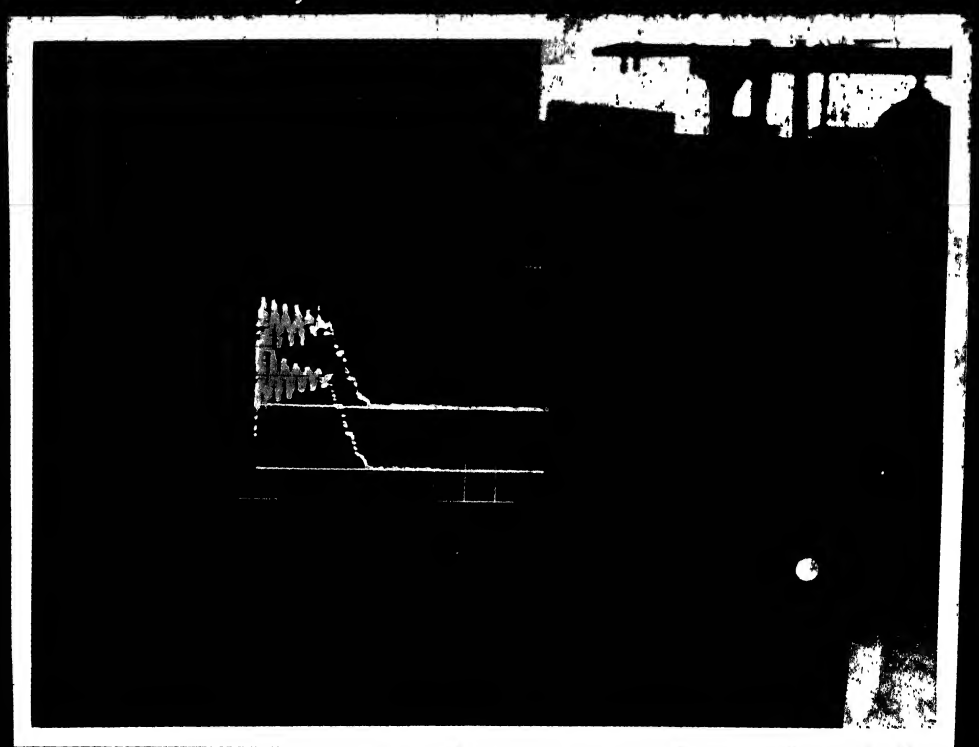

PLATE 3. Pressure-time Trace as obtained at two points in the plate

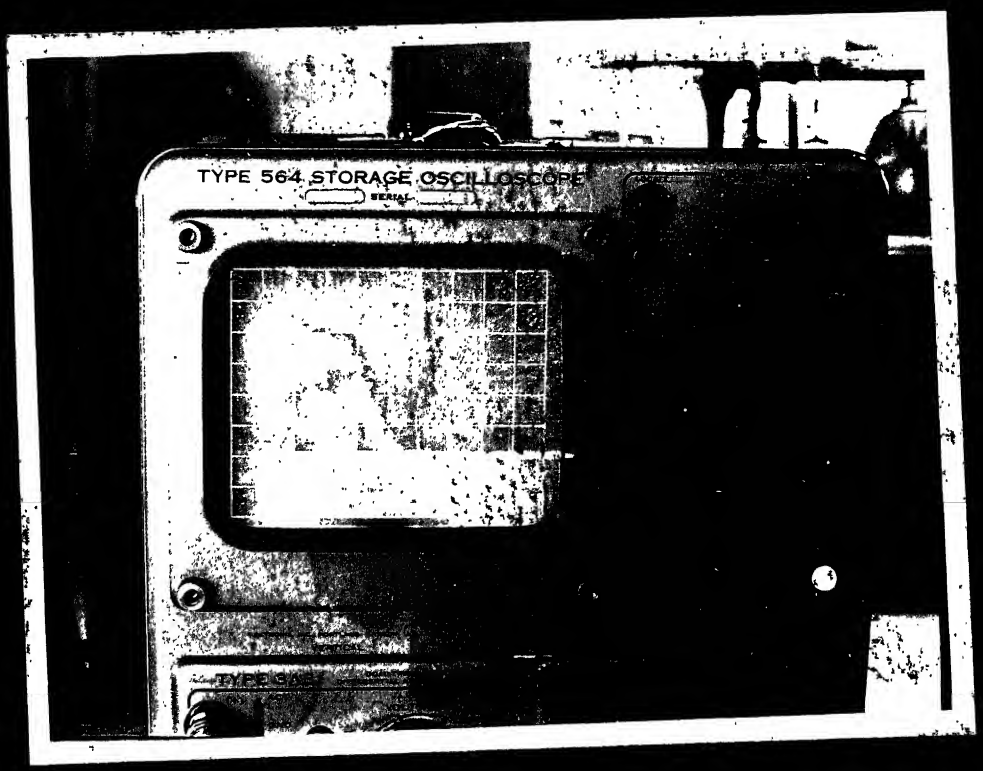

PLATE 4. Pressure-time trace

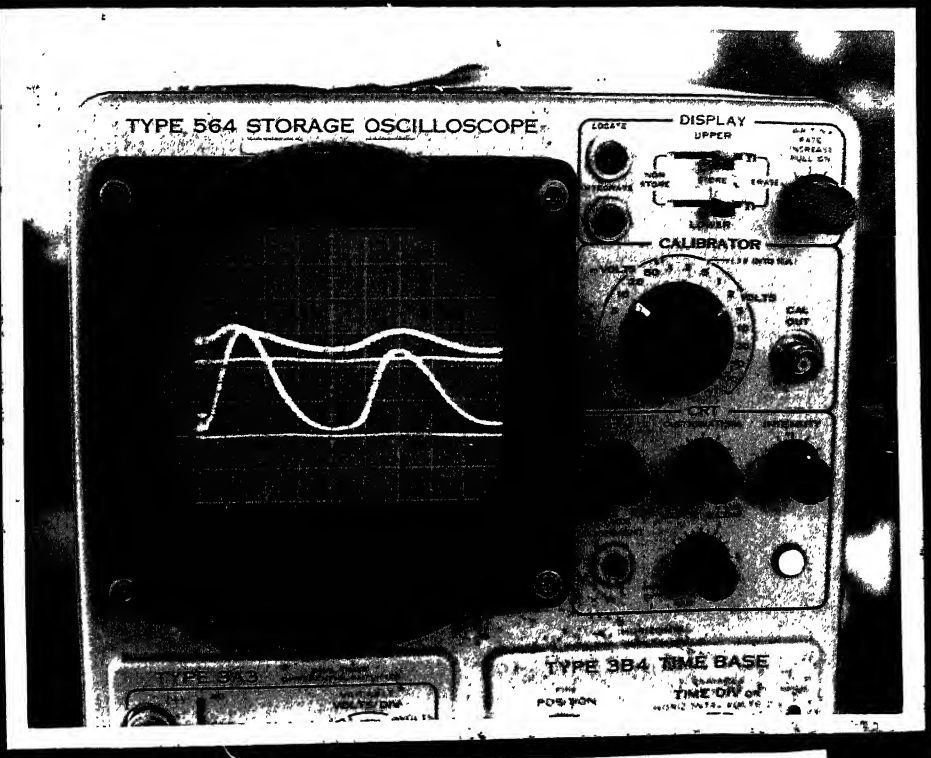

PLATE 6. Strain time trace